PMTurkeyCOLPEm Resource

From: Comar, Manny
Sent: Thursday, November 01, 2012 5:06 PM
To: TurkeyCOL Resource
Subject: FW: DRAFT RAI Responses FPL Turkey Point 6 & 7 for eRAI 6024 Basic Geologic and Seismic Information - Part 2 of 4
Attachments: Draft Revised Response for NRC RAI Letter No. 041, RAI 02.05.01-18 (eRAI 6024).pdf; Draft Revised Response for NRC RAI Letter No. 041, RAI 02.05.01-17 (eRAI 6024).pdf; Draft Revised Response for NRC RAI Letter No. 041, RAI 02.05.01-12 (eRAI 6024).pdf; Draft Revised Response for NRC RAI Letter No. 041, RAI 02.05.01-22 (eRAI 6024).pdf

---

From: Franzone, Steve [mailto:Steve.Franzone@fpl.com]
Sent: Monday, September 17, 2012 8:46 PM
To: Comar, Manny
Cc: Burski, Raymond; Maher, William
Subject: DRAFT RAI Responses FPL Turkey Point 6 & 7 for eRAI 6024 Basic Geologic and Seismic Information - Part 2 of 4

Manny,

To support a future public meeting, FPL is providing draft revised responses for eRAI 6024 (RAI questions 02.05.01-12, 02.05.01-17, 02.05.01-18, 02.05.01-22) in the attached files.

DRAFT RAI Responses FPL Turkey Point 6 & 7 for eRAI 6024 Basic Geologic and Seismic Information - email 2 of 4 dated 20120917 and in the following 2 e-mail transmittals.

If you have any questions, please contact me.
Thanks
Steve Franzone
NNP Licensing Manager - COLA
" Words may show a man's wit, but actions his meaning" ~ Benjamin Franklin
561.694.3209 (office)
754.204.5996 (cell)

Hearing Identifier: TurkeyPoint_COL_Public
Email Number: 688

Mail Envelope Properties (377CB97DD54F0F4FAAC7E9FD88BCA6D0B1656EF962)

Subject: FW: DRAFT RAI Responses FPL Turkey Point 6 & 7 for eRAI 6024 Basic Geologic and Seismic Information - Part 2 of 4
Sent Date: 11/1/2012 5:06:11 PM
Received Date: 11/1/2012 5:06:20 PM
From: Comar, Manny

Created By: Manny.Comar@nrc.gov

Recipients:
"TurkeyCOL Resource" <TurkeyCOL.Resource@nrc.gov>
Tracking Status: None

Post Office: HQCLSTR01.nrc.gov

Files	**Size**	**Date & Time**
MESSAGE	1537	11/1/2012 5:06:20 PM
Draft Revised Response for NRC RAI Letter No. 041, RAI 02.05.01-18 (eRAI 6024).pdf	1434914	
Draft Revised Response for NRC RAI Letter No. 041, RAI 02.05.01-17 (eRAI 6024).pdf	930009	
Draft Revised Response for NRC RAI Letter No. 041, RAI 02.05.01-12 (eRAI 6024).pdf	2453780	
Draft Revised Response for NRC RAI Letter No. 041, RAI 02.05.01-22 (eRAI 6024).pdf	386599	

Options
Priority: Standard
Return Notification: No
Reply Requested: No
Sensitivity: Normal
Expiration Date:
Recipients Received:

NRC RAI Letter No. PTN-RAI-LTR-041

SRP Section: 02.05.01 - Basic Geologic and Seismic Information

QUESTIONS from Geosciences and Geotechnical Engineering Branch 2 (RGS2)

NRC RAI Number: 02.05.01-18 (eRAI 6024)

FSAR Figures 2.5.1-274 through 278 and 280, 281, and 287 shows annotated seismic sections, however the staff notes that more information is needed in order to evaluate the relative ages of deformation shown in these seismic cross sections.

In order for the staff to fully understand the regional site geology area and in support of 10 CFR 100.23, please indicate the ages and formation names, if known, of the various sedimentary strata on these figures. Please clarify what is the interpreted depth to faulted strata.

FPL RESPONSE:

This response provides revised FSAR Figures 2.5.1-274 through -278, -280, -281, and -287. These figures are revised to show additional information, including seismic sequence designations and ages of faulted strata, where known. Formation names are discussed in the response text when identified by the original authors. All annotations added by FPL reflect the interpretations of the original authors, with the exception of the depth to faulted strata (in either meters or seconds). The authors typically do not describe depth to faulted strata in their papers, and therefore, FPL estimated depths from the published figures. Table 1 summarizes the information below using the best estimate of the depth from the original seismic sections. Depth is provided in meters if the original seismic section provided a depth conversion on the scale; otherwise, it is provided in seconds (two-way travel time). No attempt was made to convert two-way travel time to meters. It should be noted that these estimated depths are approximate, considering the vertical scale of the figures printed in the publications (in some cases on the order of 1:20,000).

Figure 2.5.1-274

The seismic line in FSAR Figure 2.5.1-274 is from FSAR 2.5.1 Reference 785, hereafter referred to as Austin et al. (1988). Austin et al. (1988) identify 10 prominent seismic sequence boundaries above a mid-Cretaceous (?) target horizon; however, these sequences are not correlated with individual geologic formations. They interpret this target horizon as a buried shallow-water carbonate platform, with an Albian-Cenomanian (mid-Cretaceous) age. Similarly, Sheridan et al. (1981) (FSAR 2.5.1 Reference 424) hypothesize that this platform is mid-Cretaceous in age.

The only age information provided by Austin et al. (1988) for the prominent seismic sequence boundaries above the target horizon is for the 8/9 boundary (upper reflector in Figure 2.5.1-274, Figure 14 from Austin et al. (1988)), which is the only well-sampled part of the section at Site 626. They correlate the debris flows and turbidites sampled there with the Great Abaco Member of the Blake Ridge Formation, which would mean sequence 9 is composed of middle Miocene deposits. Austin et al. (1988) note that consistent fault offset is only seen at the sequence 1/2 boundary. One of these faults is interpreted to almost reach the 2/3 boundary, which lies at a depth of 1.74 kilometers (1.08 miles) beneath sea

level and roughly 940 meters (3080 feet) beneath the seafloor (assuming a mean water depth of 800 meters (2620 feet), see Table 5 and Figure 13 from Austin et al. 1988). This faulting occurred between the deposition of mid-Cretaceous and middle Miocene sequences.

The revised annotated figure is presented in the Associated COLA Revisions section.

Figure 2.5.1-275

FSAR Figure 2.5.1-275 shows a seismic section from FSAR 2.5.1 Reference 791, hereafter referred to as Van Buren and Mullins (1983), depicting the Walkers Cay fault and four seismic sequences NLBB-1 (youngest) through NLBB-4 (oldest). These seismic sequences are not correlated with individual geologic formations. RAI response 2.5.1-14 also discusses the Walkers Cay fault and Figures 2.5.1−275, -276, and -277.

Van Buren and Mullins (1983) interpret layer NLBB-4 as shallow-water platform interior carbonates ranging in age from Santonian to mid-Cenomanian, which they correlate to the 83.5 Ma boundary between Santonian and Campanian limestones. This is also the top of sequence BP-4 from Shipley et al. (1978), which contains Santonian to mid-Cenomanian strata.

Van Buren and Mullins (1983) correlate layer NLBB-3 with sequence BP-3 of Shipley et al. (1978), containing Campanian to Maestrictian sediments (approximately 83.5 Ma to 65.5 Ma, according to Van Buren and Mullins 1983, Figure 6). Shipley et al. (1978) describe sequence BP-3 as outer shelf slope to open marine fine-grained carbonates.

Van Buren and Mullins (1983) interpret layer NLBB-2 as fine-grained periplatform oozes and lower-slope submarine slide/sedimentary gravity deposits. Van Buren and Mullins (1983) correlate the unconformity at the top of Layer NLBB-2 with the late Oligocene drop in sea level (approximately 30 Ma), which would mean it corresponds to the Paleocene to late-Oligocene sequence BP-2 of Shipley et al. (1978).

Van Buren and Mullins (1983) interpret layer NLBB-1 as slope-front fill facies consisting of fine-grained periplatform oozes and lower slope proximal to distal sediment gravity flow deposits, which is consistent with core samples. Van Buren and Mullins (1983) date this layer as Late Oligocene to Recent, but they do not formally correlate to strata defined by Shipley et al. (1978) in the text of their paper. However, Figure 6 from Van Buren and Mullins (1983) shows NLBB-1 corresponding to BP-1 from Shipley et al. (1978).

Van Buren and Mullins (1983) do not provide specific constraints on the upward termination of faulting in their text or figures. The base of NLBB-1 is clearly offset in Figure 2.5.1-275, and the authors note evidence for recurrent faulting within this sequence. However, Van Buren and Mullins (1983) also depict two continuous, apparently unfaulted, reflectors immediately above the fault in a line drawing of the upper half of the thickness of the Late Oligocene to Recent sedimentary package (NLBB-1). The fault tip, as dashed by Van Buren and Mullins (1983), is located within the middle portion of layer NLBB-1, approximately 100 meters (330 feet) below the seafloor.

The revised annotated figure is presented in the Associated COLA Revisions section.

Figure 2.5.1-276

FSAR Figure 2.5.1-276 is also taken from Van Buren and Mullins (1983) and includes the same stratigraphy as Figure 2.5.1-275. Depth to faulted strata is difficult to discern as much of the faulting in this figure is speculative (drawn with dashed lines), and no reflectors are depicted in the uppermost portion of the line drawing by Van Buren and Mullins (1983). Given this, FPL can only state that these faults penetrate the lower portion of NLBB-1, but a precise upward termination cannot be estimated. Four faults are depicted by Van Buren and Mullins (1983) in Figure 2.5.1-276 as offsetting the base of layer NLBB-1 (uppermost reflector) and upward into the late Oligocene to Recent section. The westernmost fault intersects the base of layer NLBB-1 at an approximate depth of 110 meters (360

feet) beneath the seafloor; however, the authors extend the fault as a dashed line to within 25 meters (82 feet) of the seafloor.

The revised annotated figure is presented in the Associated COLA Revisions section.

Figure 2.5.1-277

Austin et al. (1988) identify seven seismic stratigraphic sequences that they label A through G (top to bottom). These seismic sequences are not correlated with individual geologic formations. Comparing to other studies, Austin et al. (1988, p. 394) indicate that their F/G boundary corresponds to the NLBB-3/4 boundary of Van Buren and Mullins (Table 1 of Van Buren and Mullins 1983), marking the top of the uppermost Albian shallow-water platform carbonates sampled at Site 627 (Austin et al. 1986a). Above this, Austin et al.'s (1988) seismic sequence boundary C/D is correlated with the boundary between latest early Miocene debris flows and Early Paleocene to Early Miocene limestone at Site 627 (Austin et al. 1986a). Based on depth and seismic velocity comparisons, the C/D boundary of Austin et al. (1988, Figure 5) corresponds to the NLBB-1/2 boundary from Van Buren and Mullins (1983). Austin et al. (1988, p. 395) note that "the distinct vertical facies succession" clearly observable in LBB 17 and LBB 18 is "more chaotic" at LBB 13. Thus, the C/D boundary (and to a lesser extent, the F/G boundary) highlighted in red in Figure 2.5.1-277 represents a best effort by FPL to separate seismic facies.

In Figure 2.5.1-277, the authors point out the location of three fault strands on the lower part of the profile, but no faults are drawn within the profile to help assess the authors' interpretation of the shallowest faulted strata. The top of Austin et al.'s (1988) Early Cretaceous seismic sequence G is clearly offset in three relatively narrow zones, with the majority of displacement occurring on the westernmost fault splay, which is closest to the mapped trace of the Walkers Cay fault. Moving upsection along this splay, FPL interprets displacements to become smaller and spread over a greater width. In latest early Miocene and younger beds (seismic sequences A-C), monoclinal folding has disappeared, and the reflectors appear parallel, consistent with a decrease in slip with time.

Therefore, the base of C appears to constrain the upward limit of faulted strata (i.e., sequence D is the uppermost faulted unit). The depth to the bottom of sequence C (meters below sea level) is contoured in Austin et al. (1988) as shallowing along LBB-13 from approximately 1300 meters (4270 feet) in the east to 1160 meters (3810 feet) in the west. Similarly, Austin et al. (1988) contours the thickness of sequences A-C; along LBB-13, these sequences range from 250-300 meters (820-980 feet) thick.

Evidence of faulting and folding in Figure 2.5.1-277 is most evident along the western two fault strands; the stratigraphic relationships on the easternmost splay are more difficult to interpret. In several places near the identified fault trace, down-to-the-west apparent offsets are visible, and a syncline is developed above this splay at a depth of 1.5 seconds or within the C-D seismic sequences (Miocene to Eocene age strata).

The revised annotated figure is presented in the Associated COLA Revisions section.

Figure 2.5.1-278

FSAR Figure 2.5.1-278 shows a portion of a seismic line crossing the Santaren anticline published in FSAR 2.5.1 Reference 479, hereafter referred to as Masaferro et al. (2002). The authors correlated strong reflectors in their data to reflectors identified by FSAR 2.5.1 Reference 385, hereafter referred to as Eberli et al. (1997), further to the northwest. Eberli et al. (1997) dated their reflectors using biostratigraphic indicators collected from ODP Leg 166 boreholes, and Masaferro et al. (2002) adopt these ages when dating the key layers from C-M (bottom to top). Intermediate layers (C1, G1, etc.) are undated.

The ages of layers C-M are identified in FSAR figure 2.5.1-278. The ages for these layers are: C (23.7 Ma), D (23.2 Ma), E (19.2 Ma), F (16.0 Ma), G (15.1 Ma), H (12.2 Ma), I (10.1 Ma), J (9.0 Ma), K (6.2 to 8.7 Ma), L (5.6 Ma), and M (3.6 Ma). Geologic formations are not identified; instead, Masaferro et al. (2002) rely on the general characterization provided by Ball et al. (1985) (FSAR 2.5.1 Reference 501) and Eberli et al. (1997), who identify the entire sequence as mixed pelagic/hemipelagic sediments intermittently interrupted by platform-derived carbonates with varying amounts of clay.

Layer E (19.2 Ma) is identified by Masaferro et al. (2002) as the oldest layer that overlaps, rather than onlaps, the Santaren anticline and represents a transition to much lower fold growth rates FSAR Reference 426 (Masaferro et al. 1999, Figure 11a, Figure 13a and 13b, and Figure 15; Masaferro et al. 2002, Figure 3a and 3b). After deposition of layer L (5.6 Ma), individual modeled fold uplift rates are essentially zero; the largest uplift rate of 0.08 millimeters per year (0.003 inches per year) occurs in layer L2 (Masaferro et al. 2002, Figure 4c). The youngest interval for which a non-zero uplift rate was calculated was the M2-M3 interval, which has a 0.05 millimeters per year (0.002 inches per year) fold uplift rate (Masaferro et al. 2002). RAI response 2.5.1-15 discusses the uncertainties associated with these observations.

The revised annotated figure is presented in the Associated COLA Revisions section.

Figures 2.5.1-280 and 281

Figures 2.5.1-280 and 281 are seismic lines from offshore Cuba shown in FSAR Reference 497, hereafter referred to as Echevarria-Rodriguez et al. (1991). In both figures, the authors use Roman numerals to designate seismic horizons of Tertiary, Upper Cretaceous, and Upper Jurassic age. These horizons are not correlated with individual geologic formations. They do not trace these horizons, but FPL has presented a best effort at doing so in the attached annotated figure. In figure 2.5.1-280, which depicts seismic line A-A', Echevarria-Rodriguez et al. (1991) indicate that both the northern and southern faults terminate upward just below the seismic horizon labeled Tertiary, at approximately 0.7 and 0.5 seconds (two-way travel time) beneath the seafloor, respectively.

In Figure 2.5.1-281, seismic line B-B' has several faults, the youngest of which is depicted by Echevarria-Rodriguez et al. (1991) to terminate upward at the Upper Cretaceous seismic horizon, at approximately 1.2 seconds (two-way travel time) beneath the seafloor. FPL highlights this fault depicted by the authors in black, along with their best effort at tracing the Upper Cretaceous seismic horizon. FPL also notes that deformation may be interpreted just above the upper termination of this fault; however, the uppermost 0.26 seconds (two-way travel time) of this seismic section appear undeformed. No other stratigraphic information for these seismic lines is presented in Echevarria-Rodriguez et al. (1991).

The revised annotated figure is presented in the Associated COLA Revisions section.

Figure 2.5.1-287

FSAR 2.5.1 Reference 484, hereafter referred to as Moretti et al. (2003), identifies seismic reflectors A-M (bottom to top). These reflectors were correlated to the known lithostratigraphy of north-central and western Cuba using existing and newly acquired analysis of samples from western Cuba. The authors note that some of the ages they present are hypothetical, and correlation to seismic reflectors is open to debate.

Group C, the lowermost unit in Figure 2.5.1-287, is interpreted as Jurassic synrift clastic deposits. Moretti et al. (2003) assign an Oxfordian age and associate this unit with the San Cayetano Formation based on source-rock potential.

Moretti et al. (2003) interpret groups D-F as middle Oxfordian to Hauteverian postrift regional platform carbonates. Group D is divided into two sections. The lower section (D1) is correlated with the Jagua Formation, which is known to form the base of this carbonate platform in western Cuba. The suggested age is upper Oxfordian. Moretti et al. (2003) correlate the upper section (D2) with the Kimmeridgian San Vicente Formation. Group E is thought to comprise the Americano, Artemisa, and Cifuentes Formations, which span upper Kimmeridgian to Tithonian time (top Jurassic). The authors suggest Group F comprises the Tumbadero, Sumidero, and Ronda formations, spanning Berriasian to Hauteverian time.

Moretti et al. (2003) interpret groups G-J as middle Cretaceous Bahama Channel deposits. Group G is correlated with the Aptian-Albian-Early Cenomanian Pons and Carmita formations by comparing onshore and offshore drill core data. Group H is correlated with the Cenomanian/Turonian Angelica Formation based on new onshore drill core analysis. The authors propose that Group J is composed of Paleocene sediments.

Groups I-M are not discussed in the text, but Figure 2 from Moretti et al. (2003) associates these groups with relative ages. Group I is thought to be late Cretaceous, groups J, K, and L are respectively correlated with the Paleocene, Eocene, and Oligocene, and Group M is Neogene to Recent.

Numerous normal faults cut Upper Jurassic and older horizons, and three of these faults appear to reach the middle Cretaceous unconformity (MCU on revised Figure 2.5.1-287), which initiated after late Cenomanian time and continued to the Maastrichtian or later. One offshore normal fault terminates upward within Group M Miocene-Pleistocene strata, within approximately 0.12 seconds of the seafloor (two-way travel time). To the south, several faults associated with the Cuban fold and thrust belt are depicted. The seismic horizons are not traced near these structures, but the faults terminate upward between 0.3 and 0.7

seconds below the seafloor (two-way travel time). In the text, Moretti et al. (2003) describe this thrusting as Eocene in age.

The revised annotated figure is presented in the Associated COLA Revisions section.

Table 1: Summary of depth to uppermost faulted strata for seismic sections

Figure Number	Feature	Uppermost Faulted Stratigraphic Layer and Age	Approximate Depth Below Seafloor to Uppermost Faulted Strata
274	Basement faults in the eastern Straits of Florida	Seismic sequence 2, age not specified by authors	940 s (3080 feet), below 2/3 sequence boundary
275	Walkers Cay fault	NLBB-1, Late Oligocene to Recent	Fault tip dashed to within 100 meters (330 feet) of seafloor by authors
276	Walkers Cay fault	NLBB-1, Late Oligocene to Recent	Westernmost fault tip dashed to within 25 meters (82 feet) of seafloor by authors
277	Walkers Cay fault	Seismic sequence D, Early Miocene	250-300 meters (820-980 feet), although this is equivocal since the authors do not draw a fault
278	Santaren anticline	Discrete faulting is not interpreted by the authors.	Layer E (19.6 Ma) is first to overlap fold, uplift rate above Layer L (5.6 Ma) is indistinguishable from 0.
280	Offshore Cuban fold-and-thrust belt	Just below Tertiary horizon	0.5 seconds (two-way travel time)
281	Offshore Cuban fold-and-thrust belt	Just above Upper Cretaceous horizon	1.2 seconds (two-way travel time), potentially as shallow as 0.26 s
287	Offshore Cuban fold-and-thrust belt and normal faults	Cuban fold-and-thrust belt: Eocene Normal fault: Group M, Miocene to Pleistocene	Cuban fold-and-thrust belt: 0.3-0.7 seconds (two-way travel time) Normal fault: 0.12 seconds (two-way travel time)

This response is PLANT SPECIFIC.

References:

1. Austin, J. A., Schlager, W., Palmer, A. A., et al., 1986. *Proceedings Initial reports ODP Leg 101*, Chapter 6 Site 627: Southern Blake Plateau, pp. 111-212.
2. Shipley, T.H., Buffler, R.T., and Watkins, J.S., 1978. Seismic stratigraphic and geologic history of Blake Plateau and adjacent western Atlantic continental margin, *American Association of Petroleum Geologists Bulletin,* Vol. 62, pp. 792–812.

ASSOCIATED COLA REVISIONS:

FSAR Subsection 2.5.1.1.1.3.2.2 will be revised in several instances as indicated below and as indicated to the response to RAI 2.5.1-14, concerning the Walkers Cay fault.

Mesozoic Normal Faults of the Bahama Platform

As described above, the openings of the Gulf of Mexico and Atlantic Ocean led to the development of Mesozoic normal faults that extended the basement beneath the Florida and Bahama Platforms. No detailed maps of the entire subsurface Bahama Platform exist, but limited mapping of such faults has been done in conjunction with large-scale seismic surveys. For example, Austin et al. (Reference 432**785**) identify seven normal faults cutting a Cretaceous horizon in the Exuma Sound, and a seismic line in the Straits of Florida identified several minor normal faults cutting **strata above** a **mid-**Cretaceous **shallow-water carbonate platform at a depth of 940 meters below the seafloor** ~~horizon~~ (Figure 2.5.1-274). More commonly, the basement of the Bahama Platform is depicted as a series of fault blocks with syn-tectonic Triassic to Jurassic strata, draped by undeformed Cretaceous strata (Figures 2.5.1-264 and 2.5.1-243).

Santaren Anticline

The northwest-trending detachment fold that affects Cretaceous to Miocene strata and represents the northern limit of the Cuban fold-thrust belt (Reference 501) (Figure 2.5.1-229). Initial work indicated that folding initiated in the Late Cretaceous, reached maximum expression in the early Cenozoic, and experienced differential compaction in the late Cenozoic (Reference 501), a timeline consistent with the end of Cuban orogeny in the latest Eocene. Detailed analysis of the stratigraphy indicates that the syn-tectonic growth strata may range in age from Eocene to Late Pliocene. The analysis was also used to infer Pliocene or potential Quaternary activity on the structure (References 477 and 479). However, this detailed stratigraphic analysis indicates that the vast majority of uplift or shortening occurred before 20 Ma, with an average fold uplift rate of 0.03 millimeters/year characterizing the anticline after approximately 20 Ma (Reference 479). **Layer E (19.2 Ma) is the oldest layer that overlaps, rather than onlaps, the Santaren anticline, and represents a transition to much lower fold growth rates (Figure 2.5.1-278).** Most strata younger than 15 Ma drape across the fold crest maintaining constant bed thickness, but some beds do thin across the anticline (Reference 479) (Figure 2.5.1-278). **After deposition of layer L (5.6 Ma), individual modeled fold uplift rates are essentially zero; the largest uplift rate of 0.08 mm/yr occurs in layer L2 (Reference 479). The youngest interval for which a non-zero uplift rate was calculated was the M2-M3 interval, which has a 0.05 mm/yr fold uplift rate (Reference 479).** This could be the

result of intermittent fold uplift (e.g., Reference 479) or sedimentary processes, such as localized bottom-current erosion and sediment compaction (e.g., Reference 501). The preponderance of data indicate that this structure is Tertiary in age, predominantly active in the Eocene, with waning activity throughout the Miocene. The fold may be rooted in Jurassic evaporites, the Punta Allegre formation (References 307 and 477), which could account for this structure's apparent longevity without clear tectonic mechanisms.

Cuban Fold-and-Thrust Belt

North American passive margin strata are deformed in a series of north-vergent imbricate thrusts and anticlines along the northern edge of Cuba (Figures 2.5.1-248, 2.5.1-251, 2.5.1-252, 2.5.1-279, 2.5.1-280, and 2.5.1-281). These faults and folds are exposed onshore, particularly in western Cuba, but imaged with seismic data offshore, within about 20 miles (32 kilometers) of the Cuban coastline (References 221, 484, and 485) (Figure 2.5.1-248). Syn-tectonic strata of foreland and piggyback basins are well dated onshore and indicate that the thrust faulting is Eocene in age (References 220, 485, and 439). **In two offshore seismic lines, Reference 497 indicates that north-vergent thrusts terminate either above an Upper Cretaceous horizon (Figure 2.5.1-281), or just below a Tertiary horizon (Figure 2.5.1-280).** Based upon a series of north-northeast-trending seismic lines extending north from the Cuban shoreline in the Straits of Florida, Moretti et al. (Reference 484) conclude that the foreland fold and thrust belt developed in the Eocene and indicate that post-tectonic Tertiary and Quaternary sediments are undeformed by the thrusts. **For example, in Figure 2.5.1-287, seismic horizons are not traced near the imbricate thrusts, but the faults terminate upward between 0.3 and 0.7 seconds below the seafloor (two-way travel time).** Moretti et al. (Reference 484) do note occasional Miocene reactivations of either the early Tertiary thrusts or Jurassic normal faults. On the basis of well-dated Eocene syn-tectonic strata, published structural interpretations indicating unfaulted Quaternary strata above these structures offshore, and unfaulted Pleistocene and younger terraces along the northern edge of Cuba (Reference 847) (Figure 2.5.1-282), these faults are concluded to be Tertiary in age and not capable tectonic structures.
FSAR Figures 2.5.1-274, 275, 276, 277, 278, 280, 281, and 287 will be replaced with the revised figures shown below in a future revision of the FSAR.

Figure 2.5.1-274 Interpreted Versions of the Southern Half of Profile FS-08 in the Straits of Florida

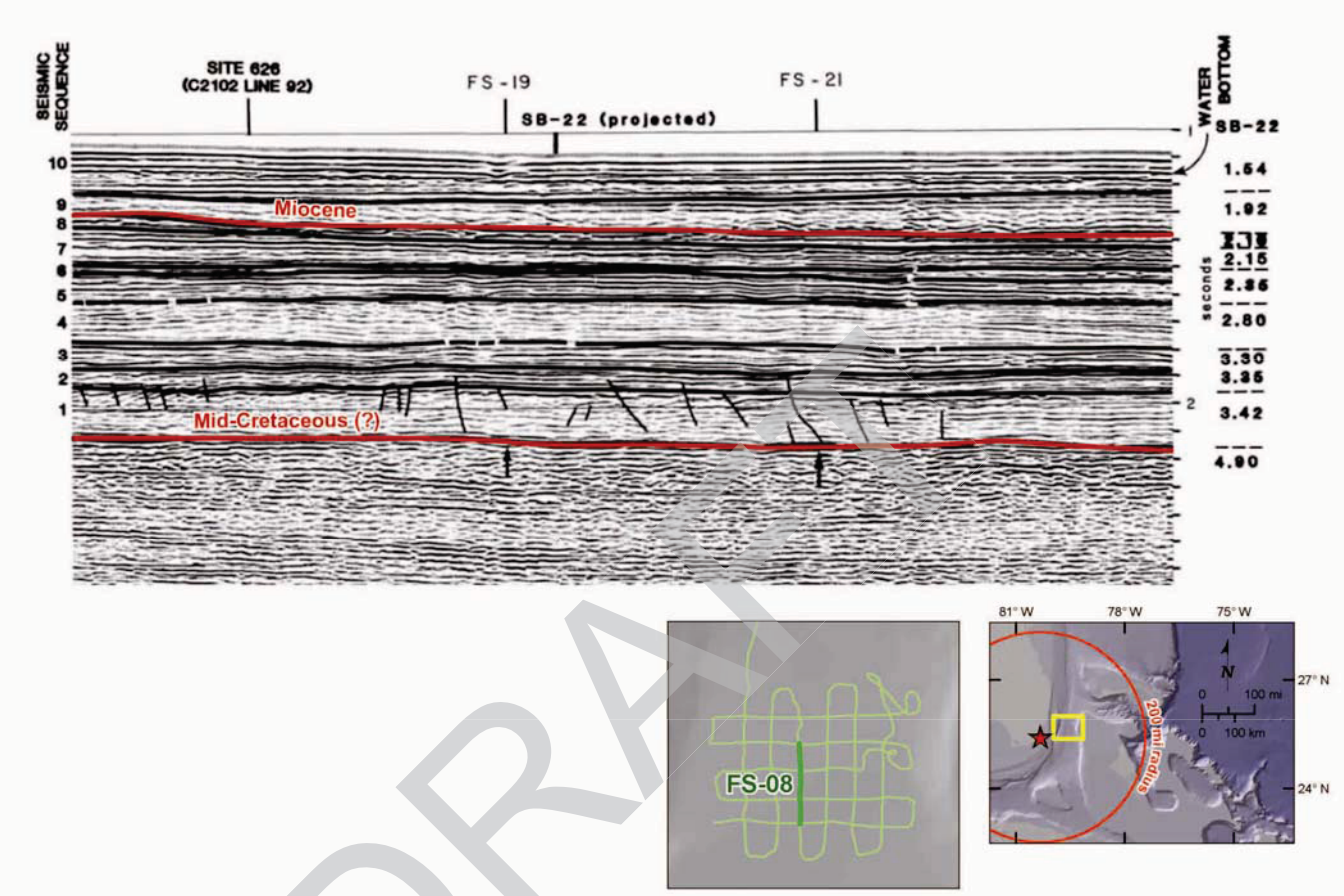

Note: Red star denotes Turkey Point Units 6 & 7.
Modified from: Reference 785

Figure 2.5.1-275 Seismic Line and Interpretation across the Walkers Cay Fault

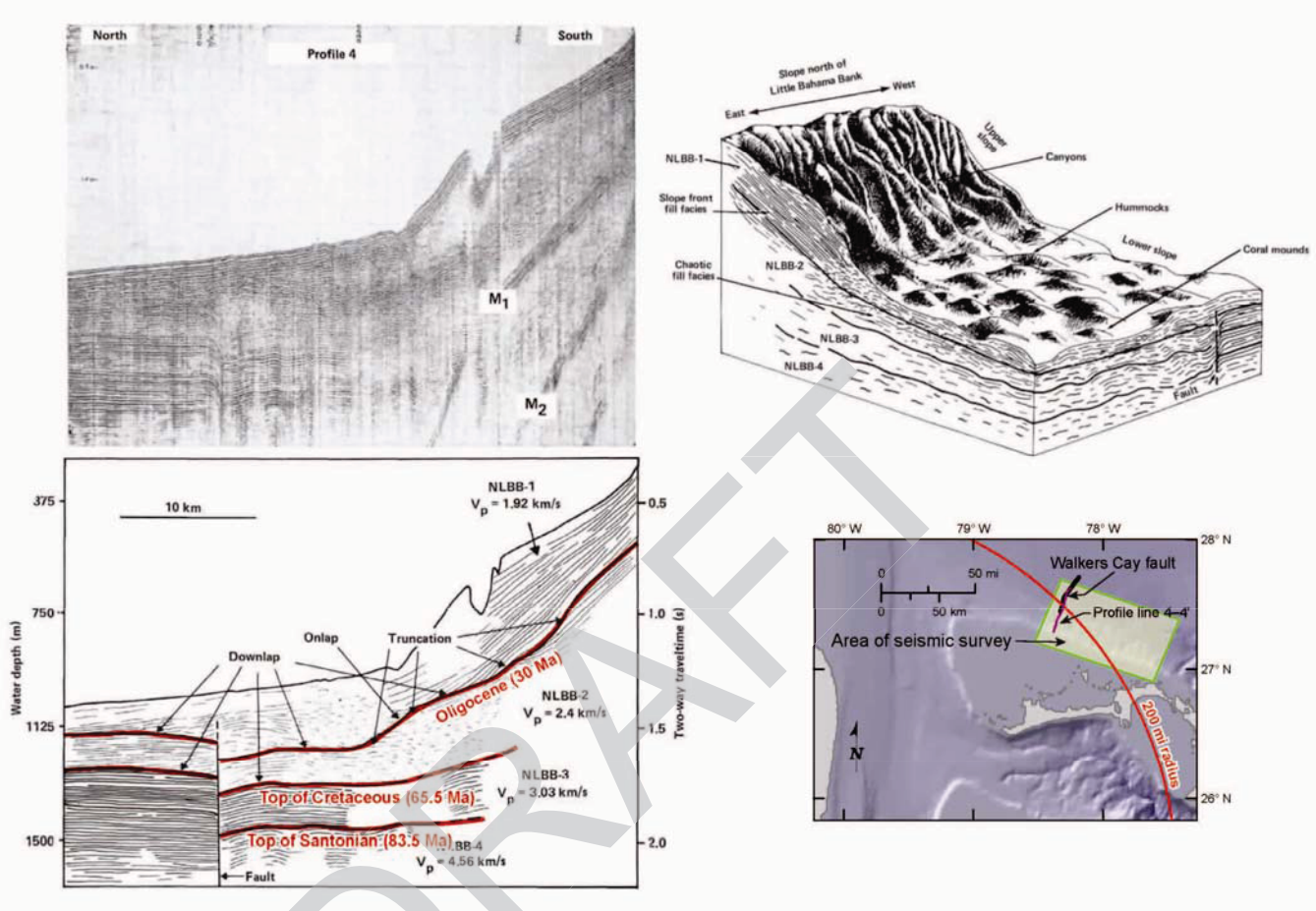

Modified from: Reference 791

Figure 2.5.1-276 Seismic Line and Interpretation across the Walkers Cay Fault

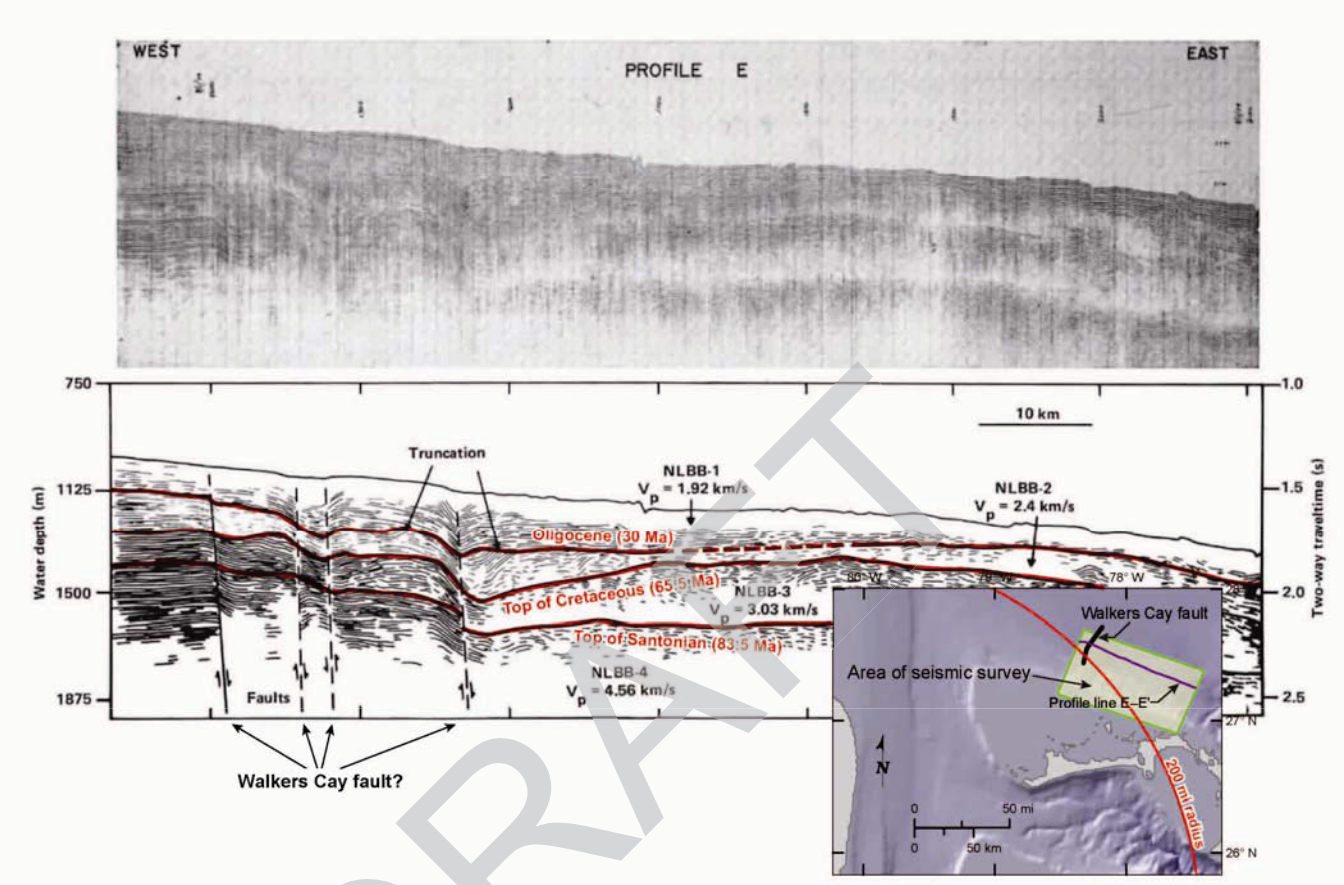

Source: Reference 791

Figure 2.5.1-277 Seismic Line along Edge of Little Bahama Bank and Walkers Cay Fault

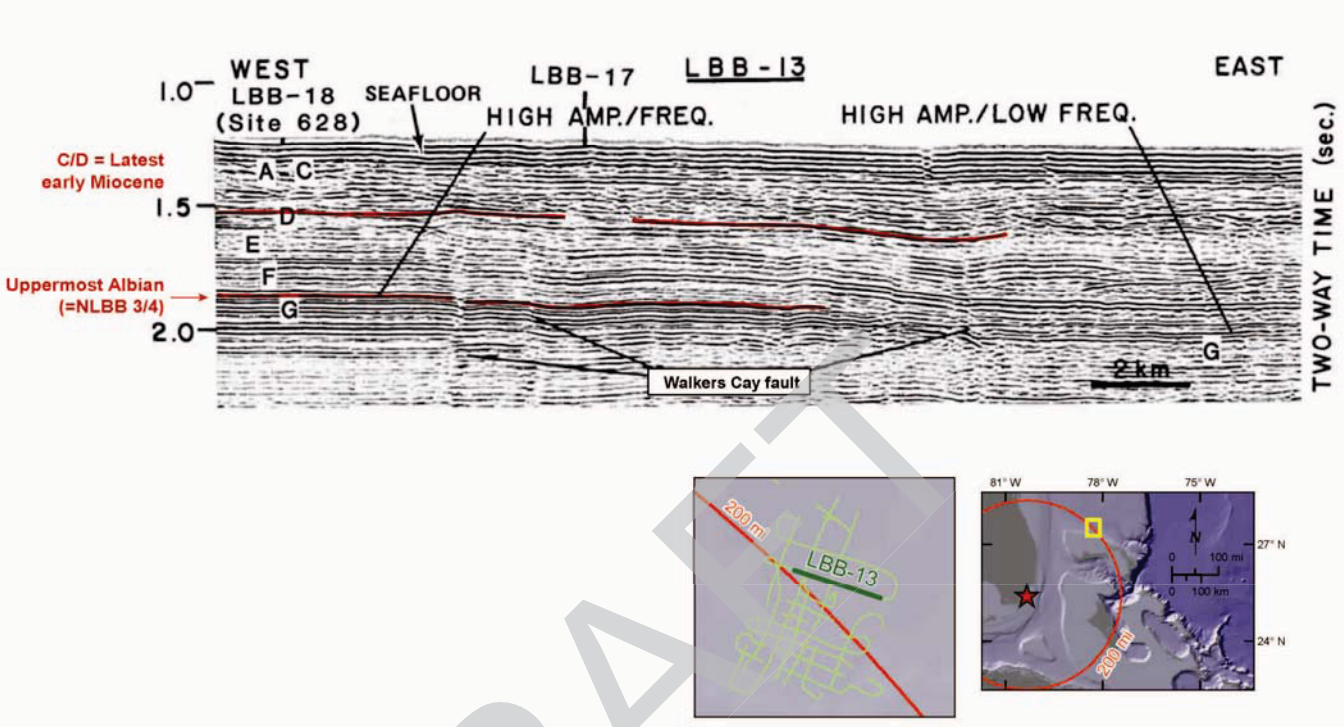

Note: Red star denotes Turkey Point Units 6 & 7.
Modified from: Reference 785

Figure 2.5.1-278 Seismic Line and Interpretation across the Santaren Anticline

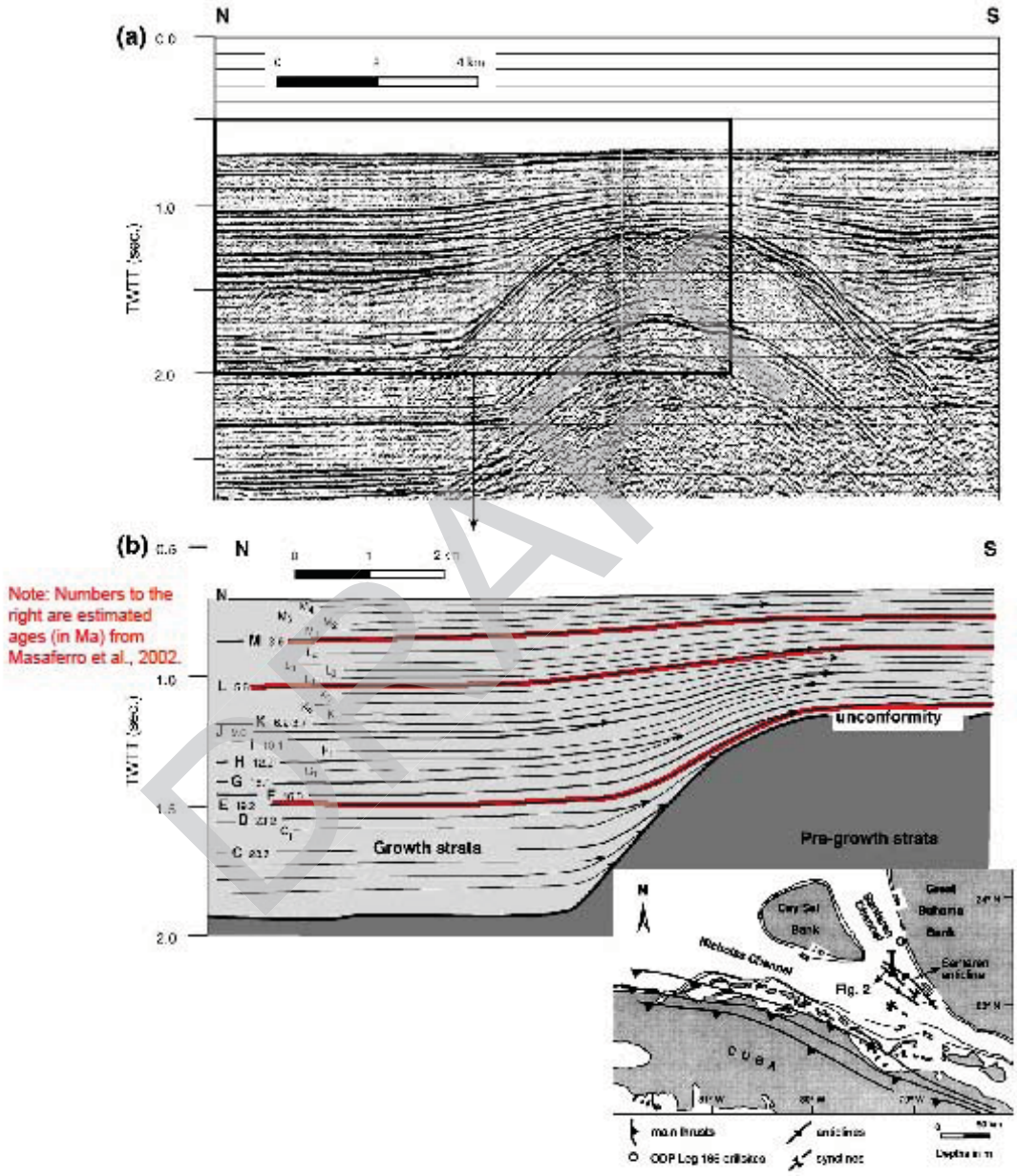

Source: Reference 479

Figure 2.5.1-280 Offshore Interpreted Seismic Line, Cuban Thrust Belt

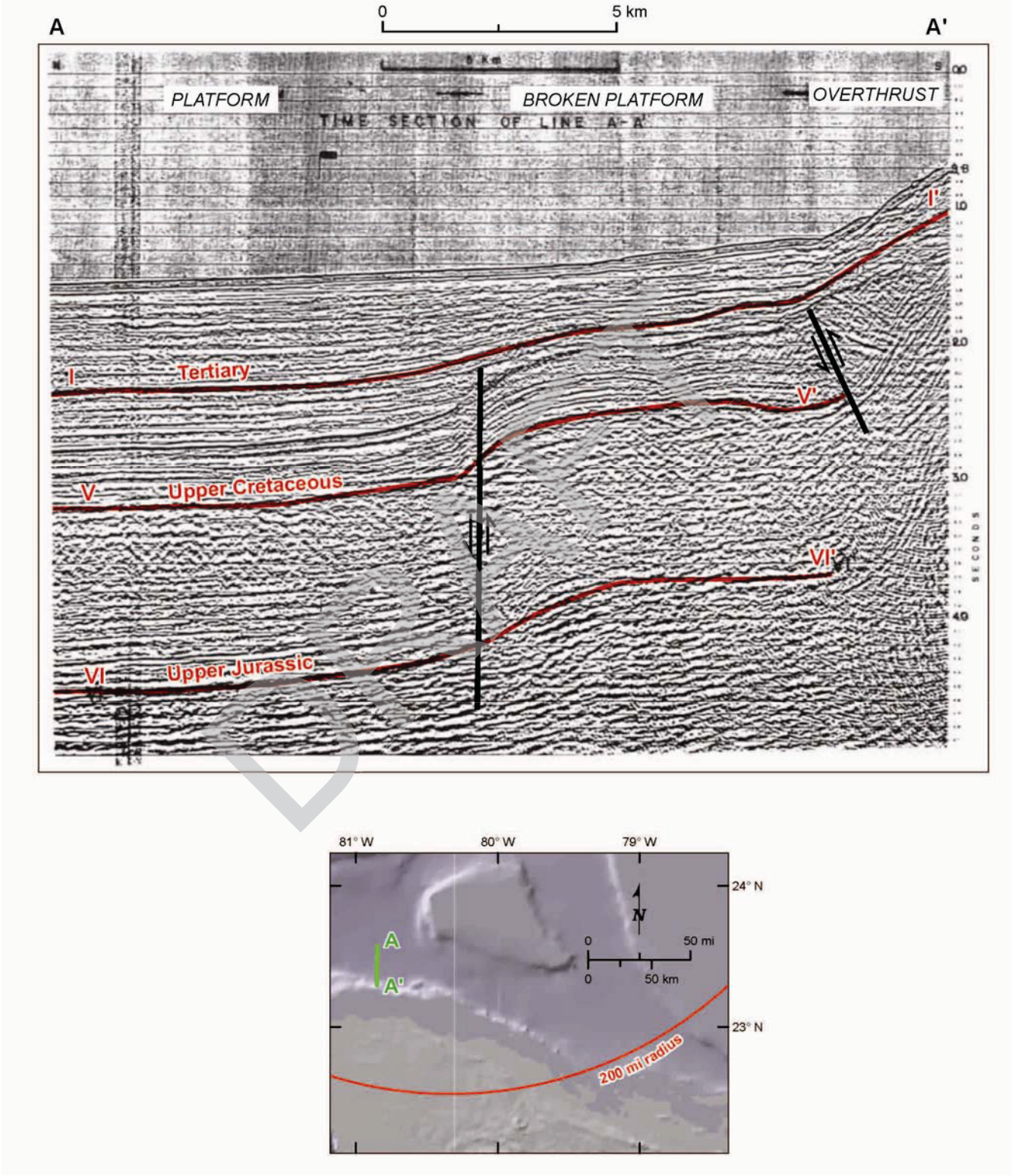

Modified from: Reference 497

Figure 2.5.1-281 Offshore Interpreted Seismic Line, Cuban Thrust Belt

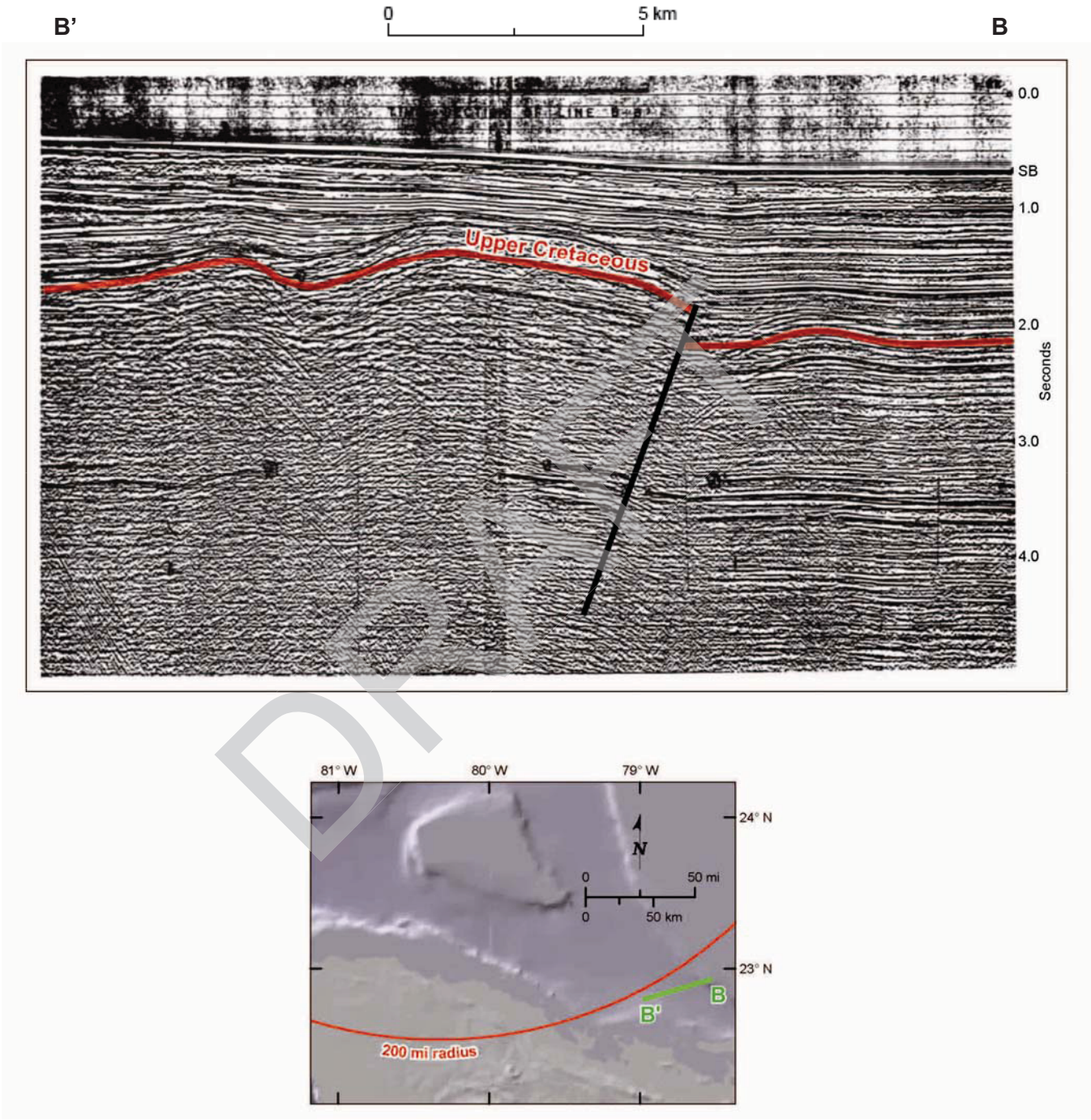

Modified from: Reference 497

Figure 2.5.1-287 Interpreted Seismic Line across Cuban Thrust Belt, Line 3A

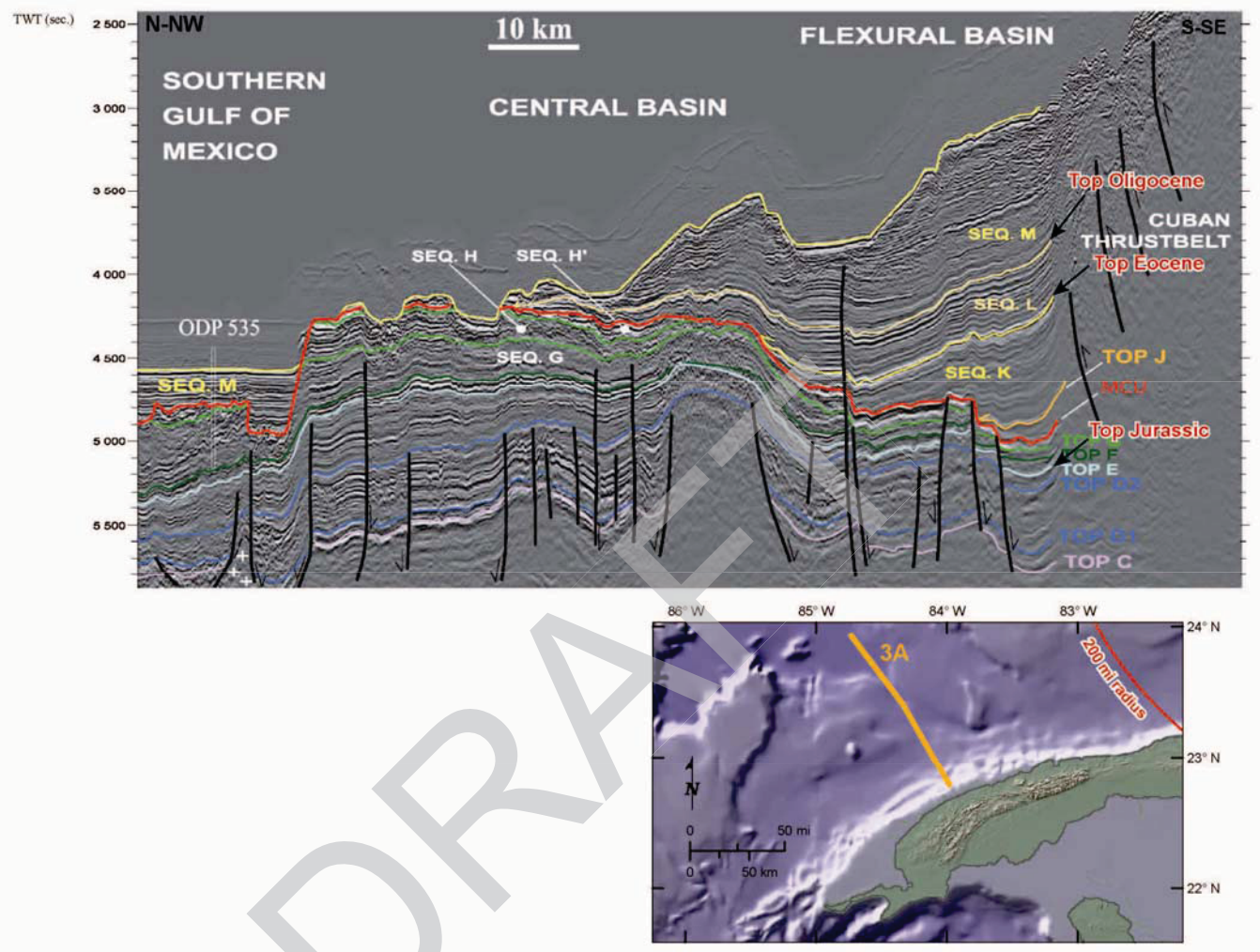

Modified from: Reference 484

ASSOCIATED ENCLOSURES:

None

NRC RAI Letter No. PTN-RAI-LTR-041

SRP Section: 02.05.01 - Basic Geologic and Seismic Information

QUESTIONS from Geosciences and Geotechnical Engineering Branch 2 (RGS2)

NRC RAI Number: 02.05.01-17 (eRAI 6024)

FSAR Figures 2.5.1-342, -343, and -344 illustrate isopach and structure contour maps of the Key Largo Limestone and Fort Thompson Limestone stratigraphic units. The staff notes, however, that additional information is needed on the maps to understand the nature of the Key Largo and Fort Thompson limestone units.

In order for the staff to evaluate depositional structures or potential tectonic deformation in the bearing layer formation within the site area and in support of 10 CFR 100.23, please address the following:

a) Indicate the elevation on the structure contour maps and thickness values on the isopachs.

b) Indicate thin areas on the isopachs and low areas on structure contours.

c) Plot the location of cross section lines A, B,C, and D on the isopach and structure contour maps.

d) Provide a structure contour for the Key Largo formation.

e) The FSAR describes the Fort Thompson Formation as vuggy, and solution-riddled. In light of this characteristic in the underlying Fort Thompson, discuss the implication of the numerous closed circles shown on the Key Largo isopach.

FPL RESPONSE:

The updated Figures 2.5.1-342, 343, and 344 and Figure 1 are provided on pages 5 though 8 of this response. Upon review of Figures 2.5.1-342, 343, and 344, it was discovered that the FSAR Figure 2.5.1-342 “Isopach of the Site: Key Largo Limestone” actually depicted the “Structure Contour Map: Top of Key Largo Limestone”. As part of this response the correct figure for “Isopach of the Site: Key Largo Limestone” is provided in the Associated COLA Revisions. Figure 1, “Structure Contour Map: Top of Key Largo Limestone”, is updated and will be added in a future revision of the FSAR as “Figure 2.5.1-349 Structure Contour Map: Top of Key Largo Limestone”.

a) The updated elevation values on the structure contour maps and updated thickness values on the isopach maps for the respective Figures 2.5.1-342, 343, and 344 and Figure 1 are provided on pages 5 through 8 of this response.

b) As shown on the updated Figure 2.5.1-342, the thickness of the Key Largo Formation ranges from about 15 to 30 feet with a minimum thickness of about 15 feet. As shown on Figure 2.5.1-344, the thickness of the Fort Thompson Formation ranges from about 60 to 70 feet.

As shown on Figure 1, the top of the Key Largo Formation ranges in elevation from about -25 to -35 feet NAVD 88, with a lower contact elevation of -35 feet NAVD 88. As shown on the updated Figure 2.5.1-343, the top of the Fort Thompson Formation ranges in elevation from about -45 to -55 feet NAVD 88, with a lower contact elevation of about -55 feet NAVD 88.

c) The location of cross section lines A, B, C, and D are plotted on the updated Figures 2.5.1-342, 343, and 344 and Figure 1.

d) The updated structure contour map for the Key Largo Formation is provided in this response as Figure 1 and will be a new figure, Figure 2.5.1-349, in a future revision of the FSAR. The updated isopach map for the Key Largo Formation is provided as FSAR Figure 2.5.1-342.

e) FPL has three interpretations for the “closed” circles in the structure contour map of the Key Largo Limestone. The first interpretation is that these are slight depressions or solution features that could have formed in a shallow patch reef environment due to sea level fluctuation during the Wisconsinan stage. The second interpretation is that the accumulation of marine organisms that compose the Key Largo Limestone were deposited in the depressions of the underlying Fort Thompson Formation. This occurred during the sea level fluctuation associated with the Wisconsinan stage. The third interpretation is surficial dissolution of the Key Largo Limestone. The formation of the slight depressions is addressed in the response to RAI 02.05.01-2 part b.

Figure 1. Structure Contour Map: Top of Key Largo Limestone

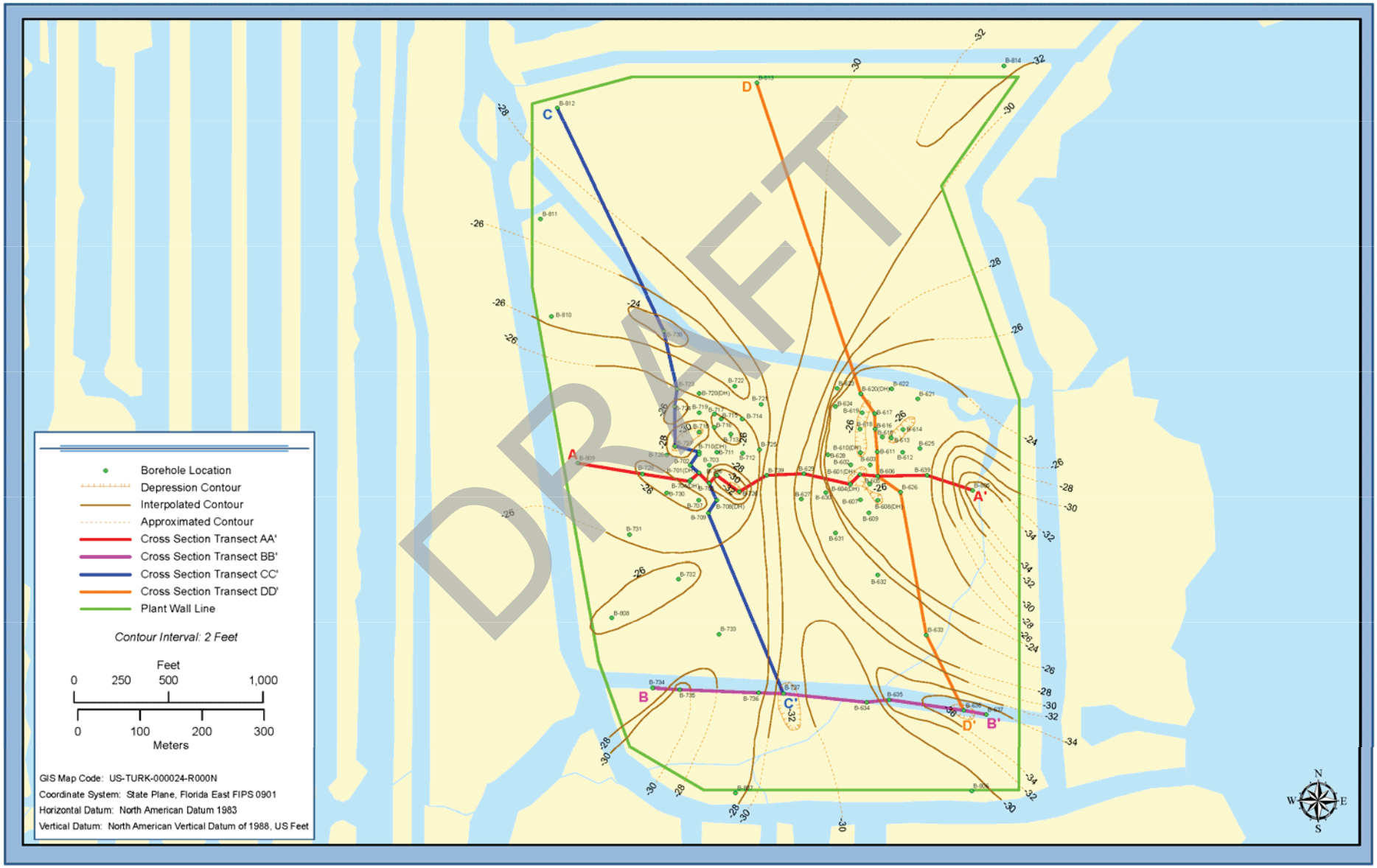

Source: FSAR 2.5.1 Reference 70

This response is PLANT SPECIFIC.

References:

None

ASSOCIATED COLA REVISIONS:

The FSAR Subsection 2.5.1, Figures 2.5.1-342, 343, and 344 will be replaced and one new figure, Figure 2.5.1-349, will be added in a future revision of the FSAR

Figure 2.5.1-342 Isopach of the Site: Key Largo Limestone

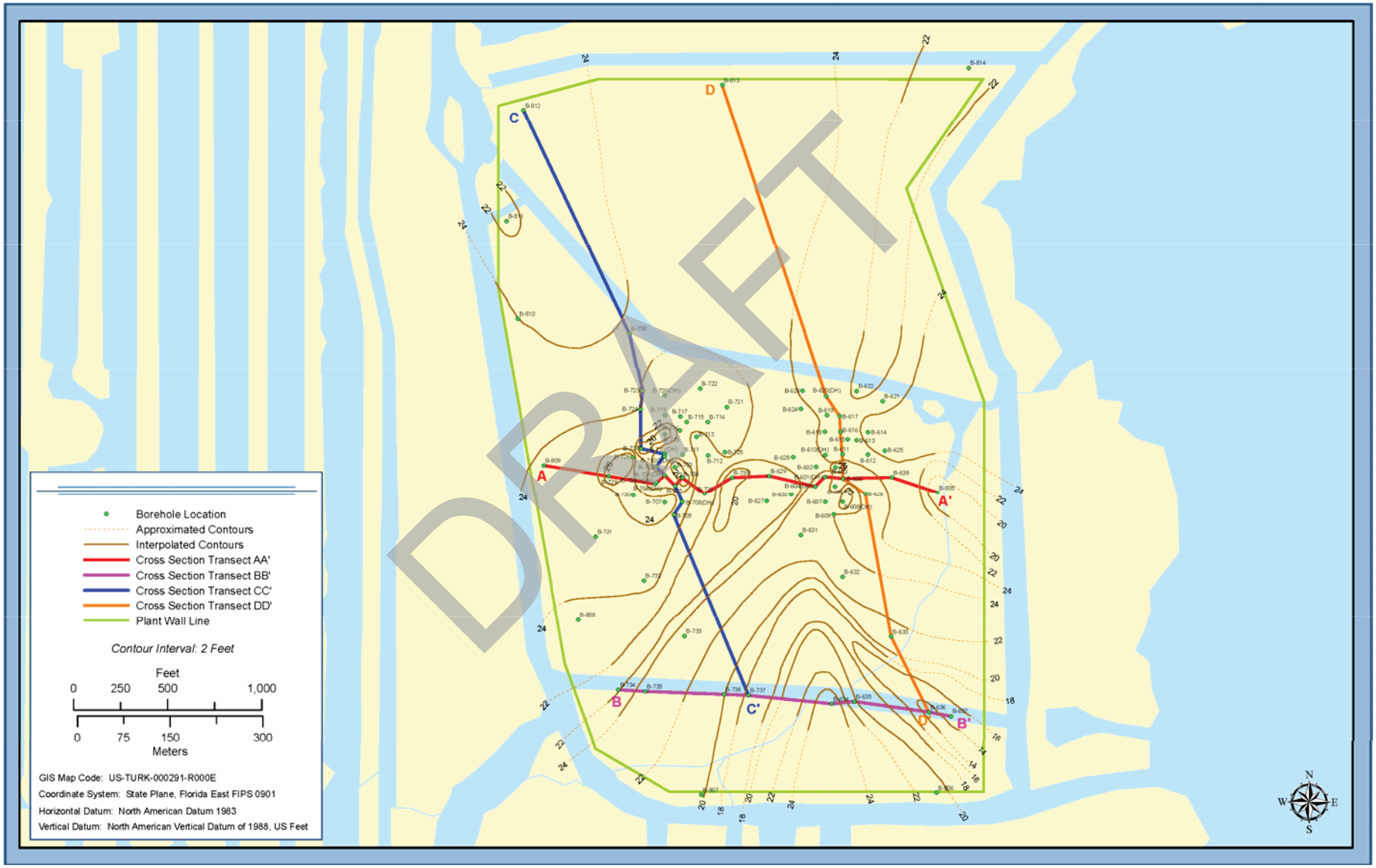

Source: Reference 708

Figure 2.5.1-343 Structure Contour Map: Top of Fort Thompson Formation

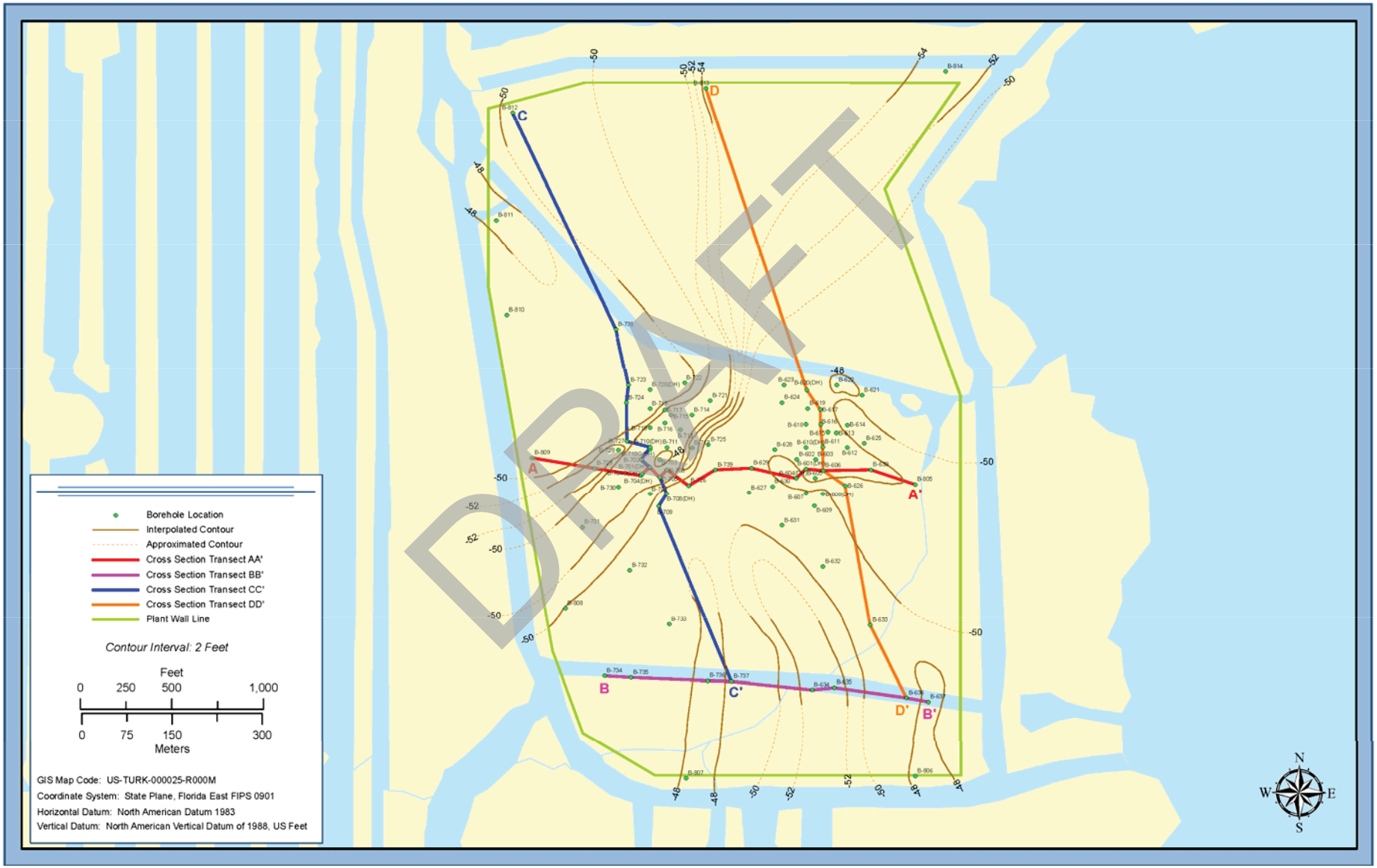

Source: Reference 708

Figure 2.5.1-344 Isopach of the Site: Fort Thompson Formation

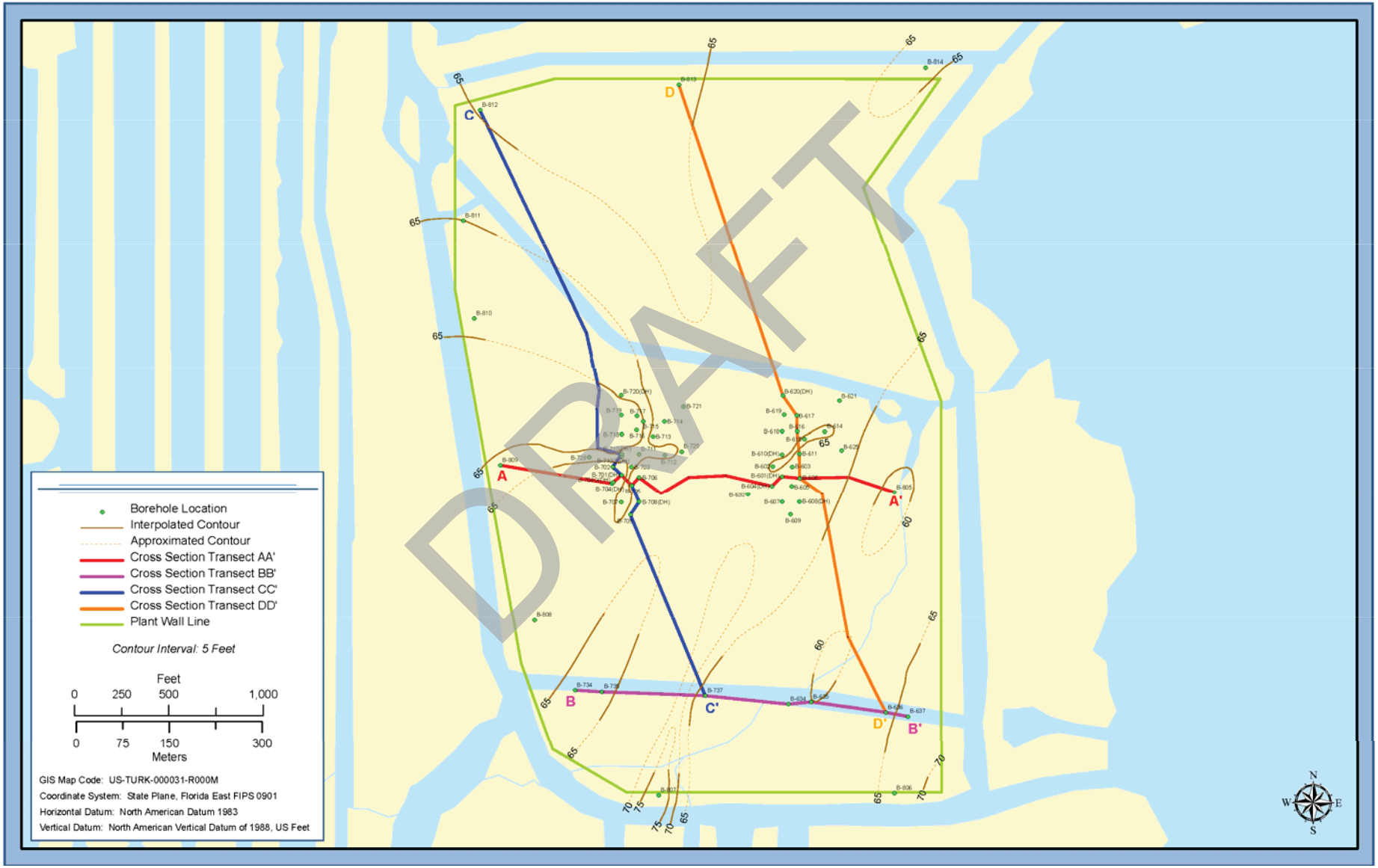

Source: Reference 708

Figure 2.5.1-349 Structure Contour Map: Top of Key Largo Limestone

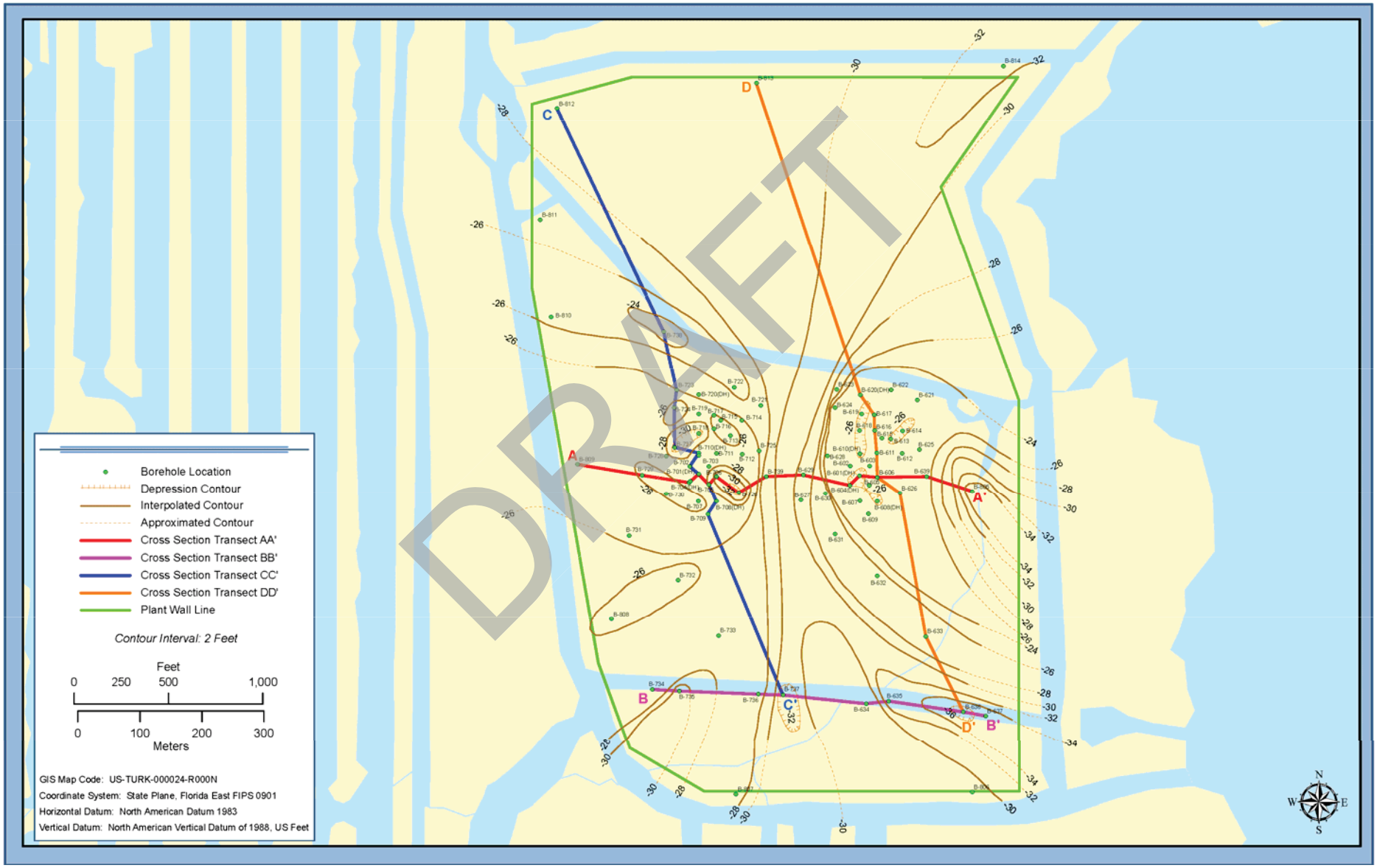

Source: Reference 708

ASSOCIATED ENCLOSURES:

None

NRC RAI Letter No. PTN-RAI-LTR-041

SRP Section: 02.05.01 - Basic Geologic and Seismic Information

QUESTIONS from Geosciences and Geotechnical Engineering Branch 2 (RGS2)

NRC RAI Number: 02.05.01-12 (eRAI 6024)

FSAR Section 2.5.1.1.1.3.2.1, "Structures of the Florida Peninsula and Platform" states that occasional variations in pre-Miocene stratigraphy recorded in boreholes due to erosion-based paleo-topography or karst have sometimes been interpreted as possible faulting; for example, the queried fault in Figure 2.5.1-234 (between wells Park W-2404 and Gulf W-3510) appears to displace the base of the Long Key and Arcadia Formations at approximately 100 m and coincides with nearly a doubling in thickness of the Long Key Formation on the downthrown (southern) side. The staff notes that the fault juxtaposes the Long Key Formation against the Arcadia Formation and the Arcadia Formation against the Avon Park Formation. Cunningham et al., 1998 (Reference 373) also provides a structural contour map of the top of the Arcadia formation and a map of net thickness of Miocene-to-Pliocene siliciclastic sand that appears to be consistent with faulting (Figure 17 of Cunningham et al., 1998). In order for the staff to fully understand site region geology and in support of 10 CFR 100.23, please address the following:

a) Substantiate your interpretation with specific evidence that the stratigraphic relations across the queried fault shown in Figure 2.5.1-234 and depicted in Reference 373 are a result of paleo-topographic or karst processes, rather than tectonic offset.
b) If the queried fault is indeed a fault, please discuss the timing and spatial extent of faulting and update the FSAR discussion accordingly.

FPL RESPONSE:

a) Substantiate your interpretation with specific evidence that the stratigraphic relations across the queried fault shown in Figure 2.5.1-234 and depicted in Reference 373 are a result of paleo-topographic or karst processes, rather than tectonic offset.

Introduction

Cunningham et al. (1998; FSAR Reference 2.5.1-373) provide three depictions of a postulated fault in southern Florida based on borehole data: a cross-section between widely spaced boreholes (Figure 1 [Figure 5 of Cunningham et al. (1998)]); structure contours on the top of the Oligocene-Miocene-age Arcadia Formation (Figure 2 [Figure 17B of Cunningham et al. (1998)]); and contoured thickness of Miocene-Pliocene siliciclastic sands (Figure 3 [Figure 17A of Cunningham et al. (1998)]).

Figure 1 is a modified version of FSAR Figure 2.5.1-234 that shows a cross-section across southern Florida (Figure 5 of Cunningham et al. [1998]). This cross-section was developed with data from eight wells in southern Florida. Between the southernmost two wells, Cunningham et al. (1998) postulate the existence of a fault that cuts up through Avon Park Formation, Suwannee Limestone, and Oligocene-Miocene-age Arcadia Formation, and potentially places the Arcadia Formation in fault contact with the lower portion of the overlying Miocene-Pliocene Long Key Formation. Alternatively, the Long Key Formation may be interpreted as deposited across a paleoscarp. Cunningham et al. (1998) label the postulated fault on this cross-section with two question marks, indicating the speculative nature of this fault. It should also be noted that Figure 1 includes a

variable horizontal scale, which necessarily results in variable vertical exaggeration throughout the cross section. Some of the greatest vertical exaggeration is in the vicinity of the postulated fault.

Figures 17A and 17B of Cunningham et al. (1998) show a dashed and queried fault on two contour maps based on well data: a structure contour map of the top of the Arcadia Formation (Figure 2) and an isopach map of Miocene-Pliocene siliciclastic sediments (Figure 3). The vertical surface projection of the queried fault shown on their contour maps (Figures 2 and 3) roughly corresponds to the location of the queried fault shown on their cross-section (Figure 1). The structure contour map of the top of the Arcadia Formation shows a circular low south of the trace of the fault, controlled by one well, Gulf W-3510, which is approximately 90 - 100 meters lower than the elevation indicated by contours north of the fault (Figure 2). The isopach map of Miocene-Pliocene siliciclastic sediments is contoured to indicate an elongate high in thickness located south of the trace of the fault (Figure 3). Both of the stratigraphic anomalies used to demarcate the fault are mostly limited to the one well south of the fault and do not include data from the wells in the Florida Keys, located more than 40 kilometers to the south. For example, the wells in the Florida Keys have Mio-Pliocene thicknesses similar to the wells north of the fault, rather than the one well immediately south of the structure (Figure 3).

Stratigraphic Data

The two wells on either side of the fault are the Everglades Park well W-2404, which drilled through the top of the Arcadia Formation northeast of the queried fault at a depth of approximately 125 meters, while to the southwest the Gulf Oil well W-3510 drilled through the top of the Arcadia Formation at a depth of approximately 225 meters. Hence, Cunningham et al.'s (1998) cross-section shows approximately 100 m of vertical separation of the top of the Oligocene-Miocene-age Arcadia Formation over a distance of approximately 18 km. As common practice in oil and gas exploration, two of the critical wells were originally logged to obtain geologic information on potential reservoirs within the Cretaceous stratigraphic section. However, Cunningham et al. (1998) use cuttings and logs archived by the Florida Geologic Survey (FGS website, 2012) to reinterpret the stratigraphy of southern Florida. Unfortunately, well W-3510, one of the key wells for the interpretation of the postulated fault, has no sampling of the Arcadia Formation from 231 - 356 meters in depth, and no samples from 375 - 505 m (FGS website, 2012).

Two Hypotheses

Although Cunningham et al. (1998) show a postulated fault in their Figures 5, 17A, and 17B (reproduced in this response as Figures 1 through 3), their figure captions do not describe the queried fault, and no specific discussion of the queried fault is provided in the text of the paper. Cunningham et al. (1998) do, however, discuss the possibility of the existence of either a "tectonically produced low" or "erosional paleotopography" (pp. 254-255):

> "A net thickness map of coarse-grained siliciclastics shows that maximum current strength for transport of the siliciclastics occurred along a corridor from west of Lake Okeechobee to the Florida Keys (Fig. 17A). This corridor of maximum current strength corresponds to a low mapped on a structural contour map on the top of the Arcadia Formation (Figure 17B). This suggests that an accumulation of the coarse-grained siliciclastics was focused within a tectonically produced low or erosional paleotopography at the top of the Arcadia. Testing this hypothesis is an objective of the SFDP [South Florida Drilling Project]. The SFDP will map the thickness of the Arcadia Formation in southern Florida and core the top of the Arcadia to

establish whether the top of the Arcadia Formation has been eroded or the Arcadia has been structurally lowered."

FPL interprets this text to indicate that Cunningham et al. (1998) consider both paleotopography and tectonic causes as equally plausible explanations for elevation variations of the top of the Arcadia Formation within southern Florida. However, FPL notes that this paragraph does not specifically describe the postulated fault on their figures. The first sentence of the paragraph on their pages 254 and 255 states that "maximum current strength for transport of the siliciclastics occurred along a corridor from west of Lake Okeechobee to the Florida Keys (Fig. 17A)". This corridor of maximum current strength, further interpreted by Cunningham et al. (1998) in the second sentence of the paragraph as a "low mapped on the structural contour map on the top of the Arcadia Formation (Figure 17B)" extends *from west of Lake Okeechobee to the Florida Keys,* and hence, a regional low oriented approximately north-south that crosses the southern portion of the Florida peninsula (similar to the grey dashed line on Figure 17B showing the "coarse-sand channel") (Figures 2 (yellow line) and 3). Without specific discussion of the queried fault drawn in Cunningham et al.'s (1998) Figures 5 and 17, FPL interprets the symbology in the figures and the general discussion on their pages 254-255 to indicate that the queried fault is offered as a speculative potential cause of thickness variations, with paleotopography being an alternate, and equally viable, possible explanation. FPL emphasizes that the Cunningham et al. (1998) paper only presents the queried structure as a possibility and is not positively identifying a fault in southern Florida.

Paleotopography

The queried fault on Cunningham et al.'s (1998) Figure 5 (FSAR Figure 2.5.1-234) is drawn to explain thickness and stratigraphic variations. These variations may instead be related to paleotopography, indeed, the top of the Arcadia Formation is known to have significant paleotopographic variation. On Key Largo, relief on the top of the Arcadia Formation as large as 40 meters was found between borings only a few kilometers apart (Warzeski et al., 1996). Futhermore, in Cunningham et al.'s (1998) Figure 4 (Figure 4), the elevation of the top of the Arcadia Formation varies by approximately 100 meters between wells W-3174 and W-17086 (88 km apart), by 50 meters between wells W-17156 and W12554 (56 km apart), and by 25 m between wells W-3011 and W-17157 (2 km apart). The slope required to achieve this latter elevation variation, 0.7 degrees, is actually greater than the slope required to achieve the elevation variation observed in the Arcadia Formation between the Everglades Park and Gulf Oil wells, where the queried fault is depicted in Figure 5 of Cunningham et al. (1998) (approximately 100 meters over 18 kilometers of distance, or a 0.3 degree slope). Numerous other examples exist throughout southern Florida of steeper paleotopographic slopes on the top of the Arcadia Formation that are not associated with faulting. In addition, the down-to-the-south separation depicted on the postulated fault in Figure 1 is consistent with, and may, in part, be attributed to the regional southward dip of the strata towards the South Florida Basin in the area (e.g., Miller, 1986; Figure 6). Similarly, the increase in the thickness of clastics south of the fault is consistent with thickness variations seen throughout southern Florida associated with proximity to the "coarse sand channel" (Figure 2).

The top of the Arcadia Formation is a known regional unconformity, which allows for the possibility of geologic thickness variations without requiring or indicating faulting (see discussion in FSAR Subsection 2.5.1.1.1.2.1.1). For example, "A distinct regional unconformity and subaerial exposure surface at the top of the Arcadia Formation separates the Long Key and Arcadia Formations" (Warzeski et al., 1996)." A cross-section presented by Warzeski et al. (1996) depicts 90 meters of

relief on the top of the Arcadia Formation surface in southern Florida, while the thickness of the Arcadia Formation varies from 200 meters in the central portion of the Florida peninsula to between 0 and 20 meters farther east (Missimer, 2001). A SFDP study in southern Florida determined that intensification of marine currents increased the erosion of marine carbonates and led to a significant time hiatus (more than 4 m.y.) following deposition of the Arcadia Formation (Guertin et al., 2000) and the influence of Arcadia Formation paleotopography on highs in subsequent carbonate and clastic deposition in southernmost Florida has been recognized (McNeil et al., 2004; FSAR Reference 2.5.1-395).

The karst-influenced paleotopography of the Arcadia Formation is detailed in Hine et al. (2009). While using borings at a much finer spacing than Cunningham study, the Hine study documents karst sub-basins with as much as 100 meters of relief over distances of kilometers to tens of kilometers on the top of the Arcadia Formation in west-central Florida. They attribute this relief to a mid to late Miocene sea-level lowstand that caused dissolution in the deeper carbonates, such as the Arcadia Formation, and formed paleotopographic depressions and non-tectonic deformation in the Arcadia Formation (Hine et al., 2009).

Faulting

Elevation variations on the top of the Arcadia Formation are hypothesized by Cunningham et al. (1998) to be the result of either faulting or erosion. Cunningham et al.'s (1998) postulated fault is depicted in their Figures 5, 17a, and 17b. FPL interprets the use of question marks on Cunningham et al.'s (1998) postulated fault as indicating those authors' uncertainty regarding the existence of this structure, and FPL interprets Cunningham et al.'s (1998) use of a dashed line in the map view to indicate where the queried fault, if it exists, is approximately located.

Alternative interpretations of well data in southern Florida, often including the three wells closest to the postulated fault, provide evidence for unfaulted Eocene to Pliocene stratigraphy in the same location (e.g., Miller, 1986; Warzeski et al., 1996; Guertin et al., 2000; Cunningham et al., 2001). For example, Figure 2 from Guertin et al. (2000) provides a stratigraphic correlation diagram across the projection of the queried fault from Cunningham et al. (1998) and interprets no faulting (Figure 5). This diagram also displays similar relief between boreholes on the top of the Arcadia to the north. Two of the co-authors of Guertin et al. (2000) also are co-authors on the Cunningham et al. (1998) publication. Likewise, the regional north-south-oriented cross-section shown in Scott (2001) intersects the projection of the queried fault and does not indicate faulting in the area (Figure 6).

As shown in Cunningham et al. (1998) Figure 17B (Figure 2), there are three wells adjacent to the queried structure: Gulf Oil W-3510 south of the postulated fault and W-1115 and W-2404 north of it. The Gulf Oil well W-3510 appears to control the set of structure contours used to delineate the area of faulting (Figure 2). Other published contour maps of the same well data use dashed contours and question marks to indicate uncertainty in contouring such sparse data in the Florida Bay area (Figures 7 and 8). A later publication, Cunningham et al. (2001), also provides interpretations of unfaulted Miocene to Pliocene stratigraphy in the same location (Figure 9) as the postulated fault from Cunningham et al. (1998). Although focused on central Florida, regional maps presented in Cunningham et al (2003) do not depict the queried fault from Cunningham et al (1998) in the same location.

Preferred Interpretation

In summary, Cunningham et al. (1998) present a dashed and queried fault as one of two possible explanations for stratigraphic variations in southern Florida. Subsequent publications by the same authors and the SFDP (e.g., Guertin et al., 2000; Cunningham et al., 2001; Cunningham et al., 2003; Hine et al., 2009) have not shown the existence of this fault in southern Florida, nor have these publications continued the postulation of the fault originally presented in Cunningham et al. (1998) (Figures 5 and 9). Because of (1) other subsequent publications excluding this fault interpretation, (2) the uncertainties associated with the tectonic interpretation of Cunningham et al. (1998), and (3) data supporting a non-tectonic origin for other similar stratigraphic variations in the region, it is more likely that paleotopography is the cause of the stratigraphic variation seen in the boreholes. Additionally, multiple alternate interpretations of well data in the area do not support the presence of faulting at the location of the queried structure presented by Cunningham et al. (1998).

b) If the queried fault is indeed a fault, please discuss the timing and spatial extent of faulting and update the FSAR discussion accordingly.

Constraints on Length of the Postulated Fault

If Cunningham et al.'s (1998) queried structure is a tectonic fault, the map indicates that the approximately located structure is between 50 and 60 kilometers long (30 - 36 miles) (Figures 2 and 3). At its nearest approach, the eastern end of the queried fault is approximately 41 kilometers (25 miles) west of the Turkey Point Units 6 and 7 site.

Constraints on Age of Most-Recent Slip on the Postulated Fault

Cunningham et al. (1998) provide no discussion of the age of most-recent slip on their postulated fault. Based on the depiction of the queried fault in Figure 5 of Cunningham et al. (1998), the fault tips out at the base of the Arcadia Formation and the Arcadia formation is potentially in fault contact with the lower portion of the overlying Miocene-Pliocene Long Key Formation (Figure 1). The depiction of potentially folded strata within the Long Key Formation (Figure 1) could be interpreted to suggest syntectonic deposition. Thus, one could interpret that movement on the postulated fault is as young as Miocene-Pliocene. Alternatively, the Long Key Formation could be interpreted as being draped over a pre-existing paleoscarp of the Oligocene-Miocene Arcardia Formation, thus post-dating slip on the postulated fault. Post-Miocene movement on the postulated fault is only suggested by Figure 17A of Cunningham et al. (1998). In this figure, Cunningham et al. draw the dashed and queried fault on an isopach map of Miocene-Pliocene siliciclastic sands (Figure 3). According to this interpretation, the postulated fault was last active during the Miocene to Pliocene, and is not a Quaternary-active structure.

In contrast, Figures 3 and 5 of Warzeski et al. (1996) depict unfaulted Miocene and younger strata in a structural contour map of the Plio-Pleistocene boundary, along with an isopach map of the Miocene Peace River Formation that indicates continuous stratigraphy across the projection of the postulated fault (Figure 7 and 8). Cunningham et al. (2001) present contour maps of Miocene and Pliocene units (e.g., Figure 9) that do not show faulting in the location of the postulated fault from Cunningham et al. (1998). Similarly, surficial maps and cross sections near the eastern portion of the postulated fault do not indicate faulting in the Pliocene and younger units (Green et al., 1996; FSAR Reference 2.5.1-830)

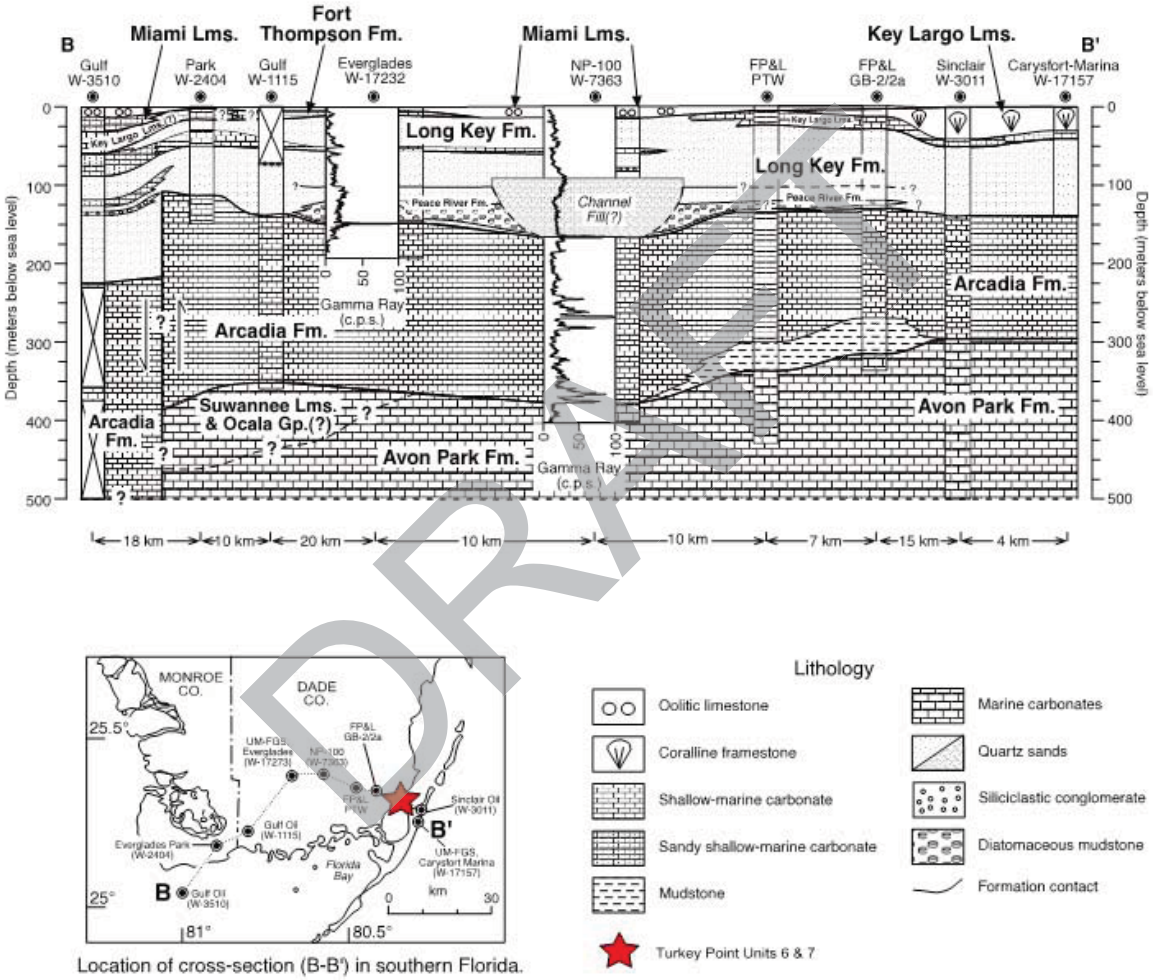

Location of cross-section (B-B') in southern Florida.

Figure 1. Figure 5 from Cunningham et al (1998); Stratigraphic correlation diagram across southern Florida.

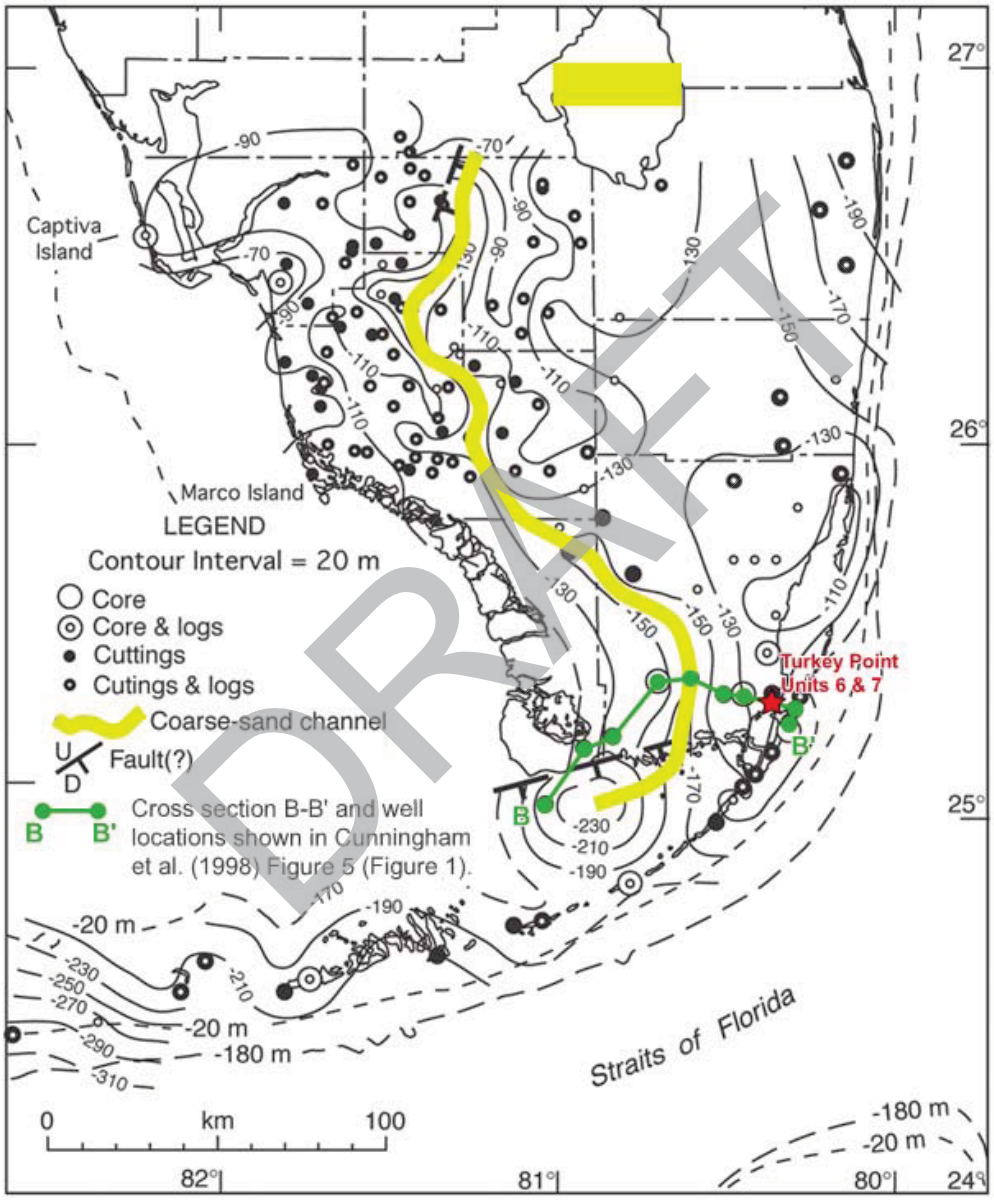

Figure 2. Figure 17b from Cunningham et al (1998); Structure contour map of the top of the Oligiocene-Miocene Arcadia formation.

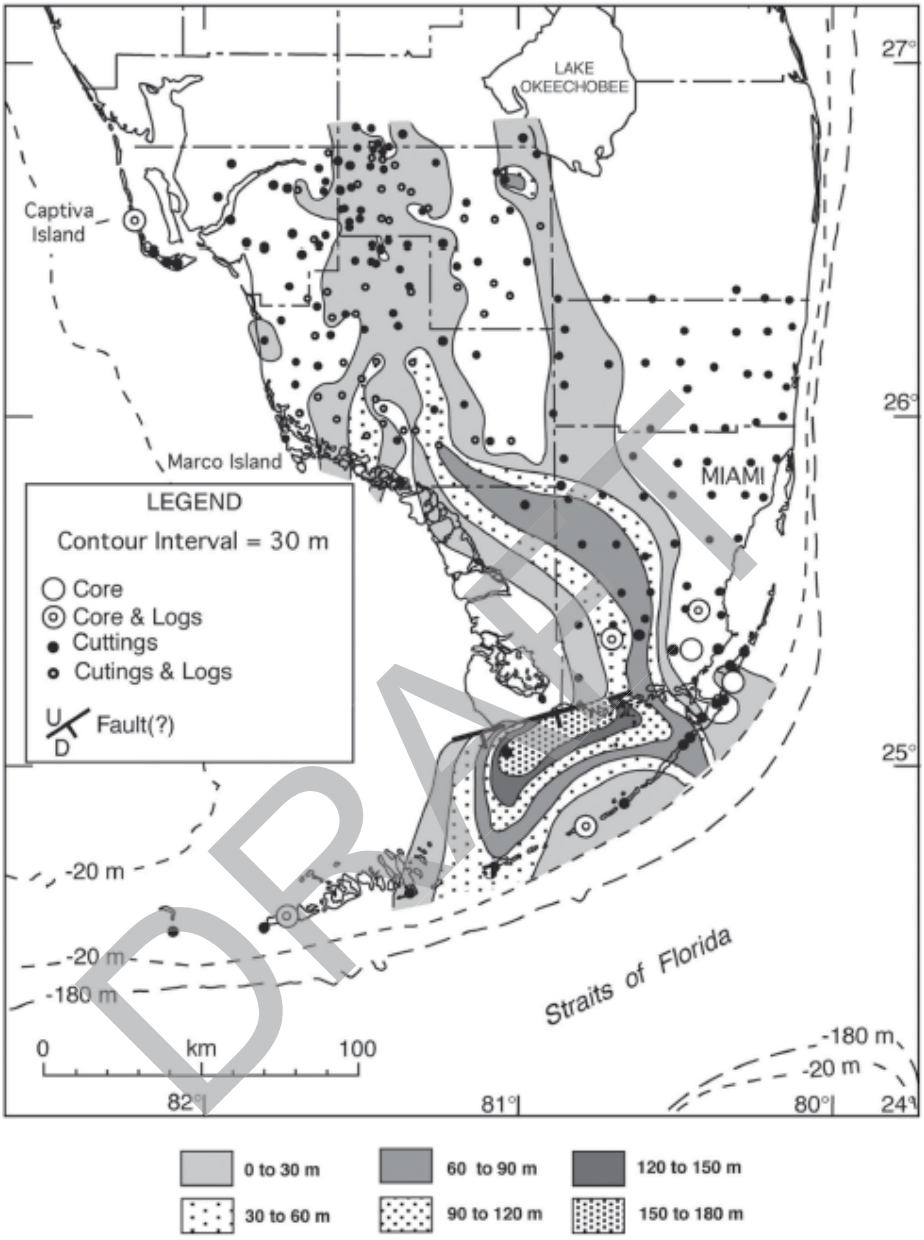

Figure 3. Figure 17a from Cunningham et al (1998); Isopach map of Mio-Pliocene silicilastic sands.

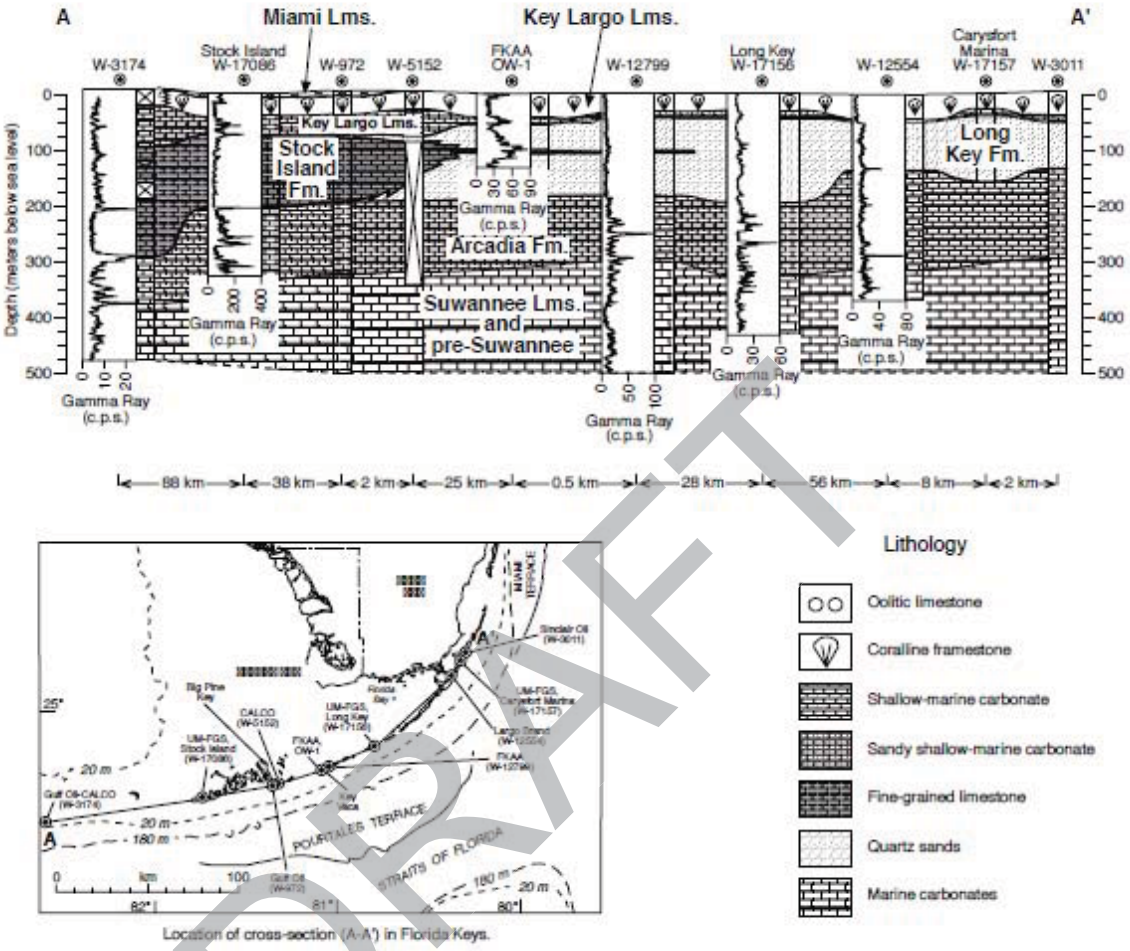

Figure 4. Figure 4 from Cunningham et al (1998); Stratigraphic correlation diagram along the Florida Keys.

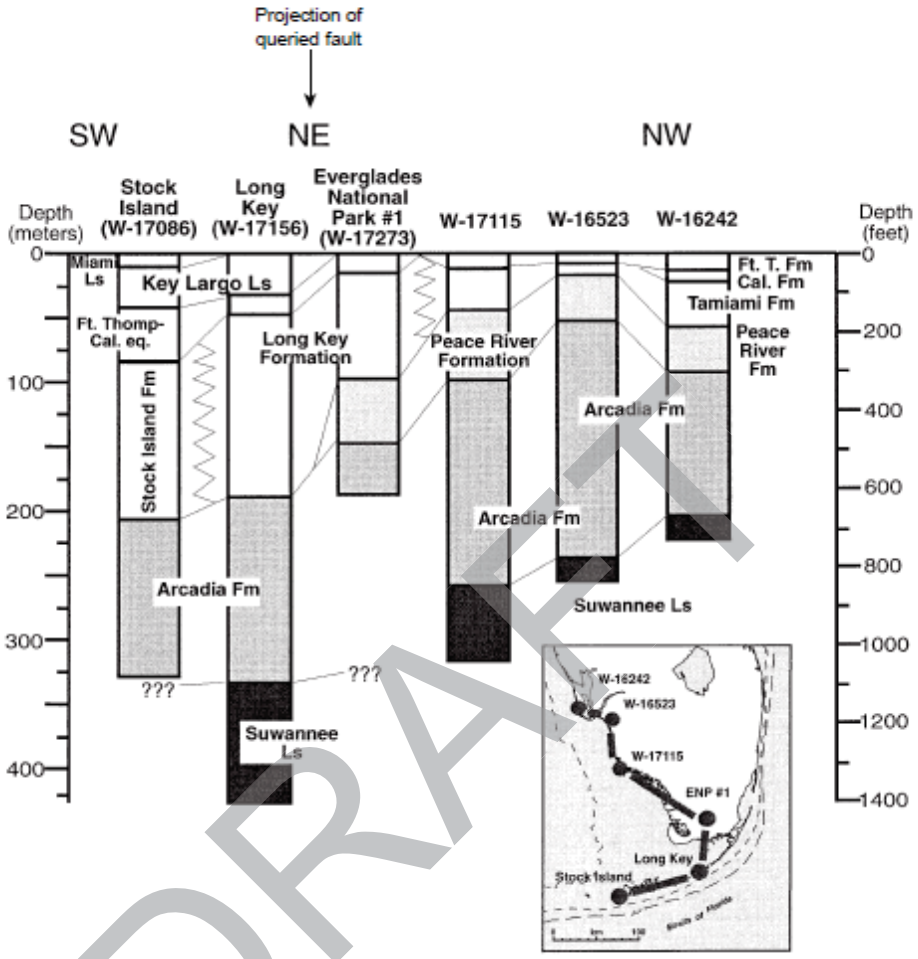

Figure 5. Figure 2 from Guertin et al (2000); Stratigraphic correlation diagram across southern Florida.

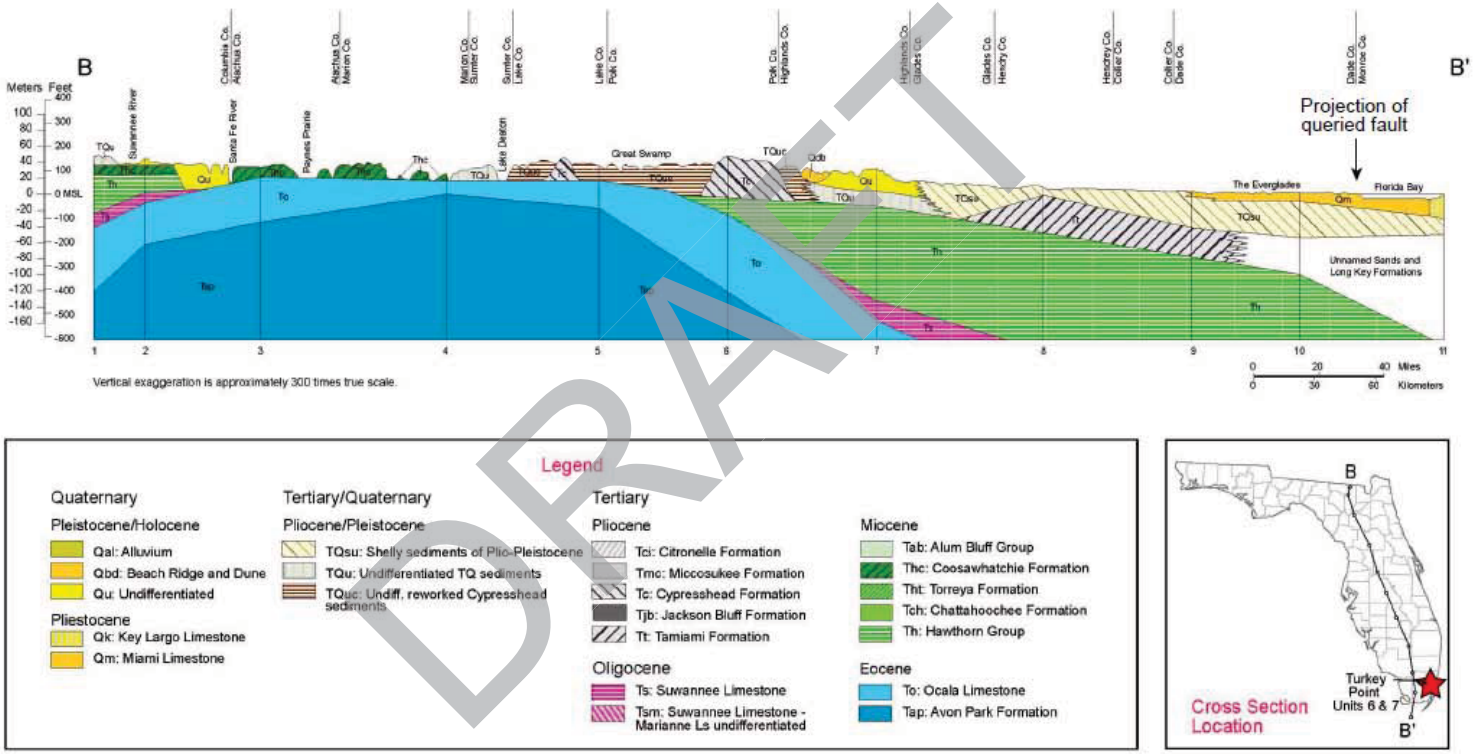

Figure 6. Figure 3 from Scott (2001); Regional north-south cross section.

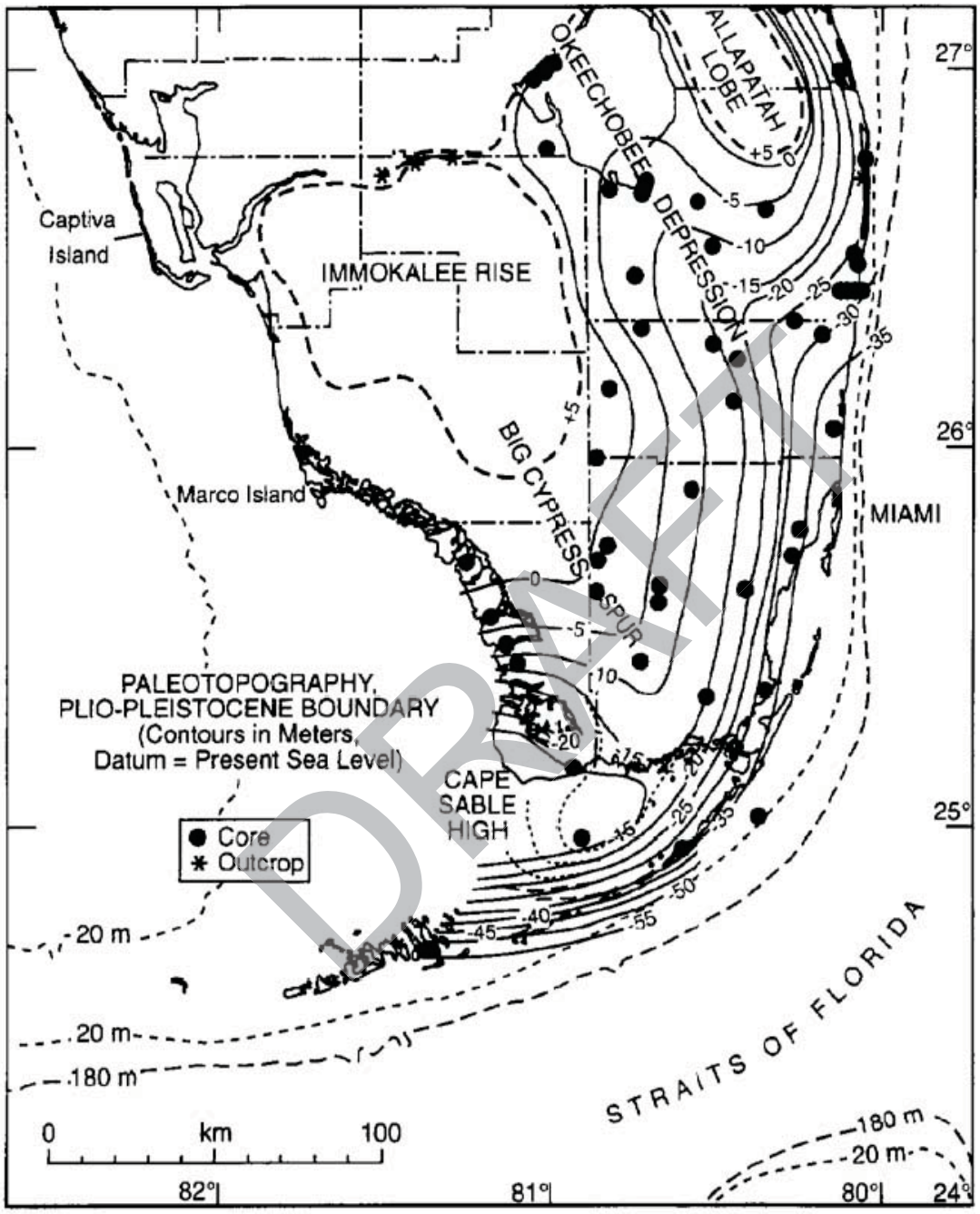

Figure 7. Figure 3 from Warzeski et al (1996); Paleotopography of Plio-Pleistocene boundary.

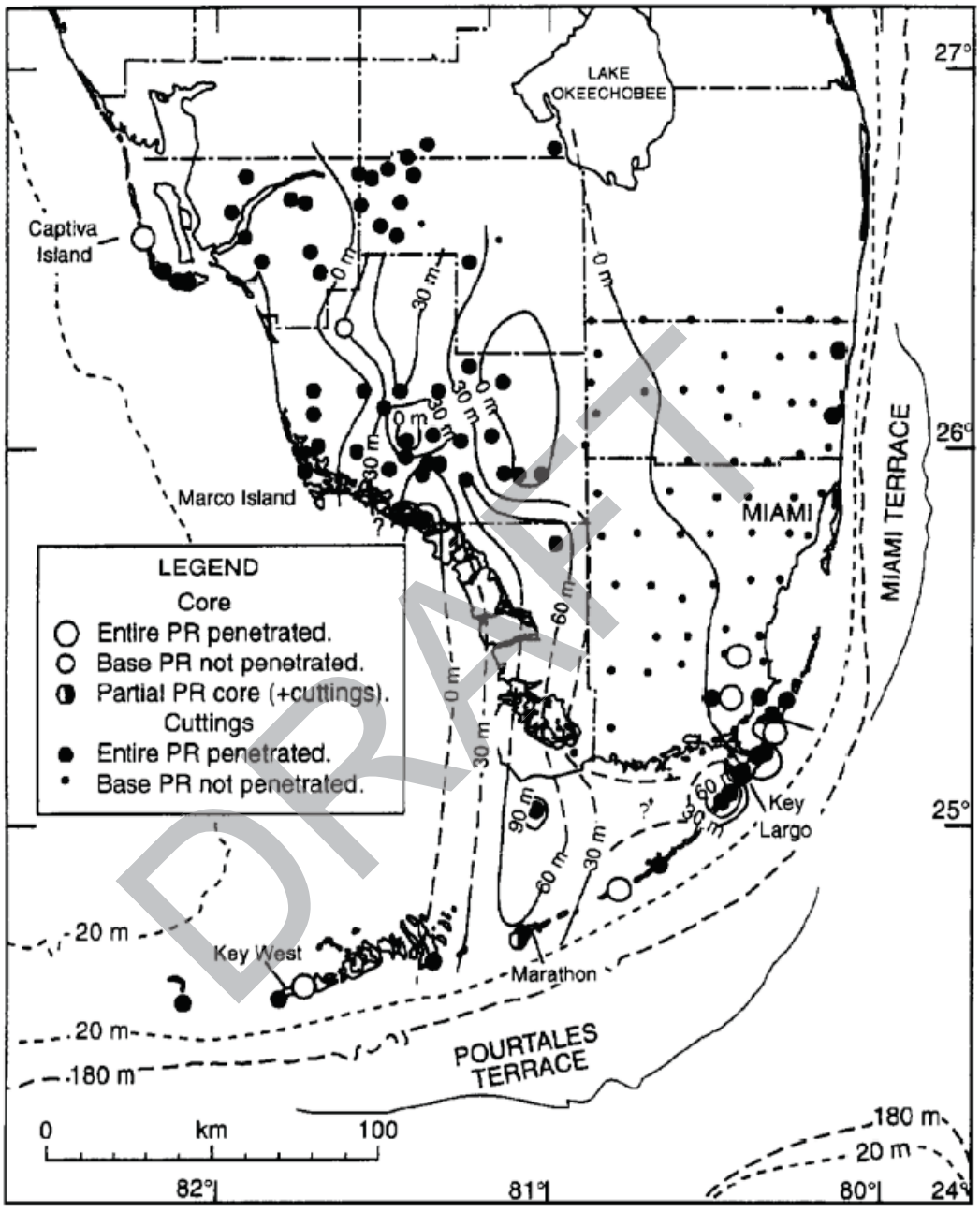

Figure 8. Figure 5 from Warzeski et al (1996); Isopach map of Miocene Peace River formation.

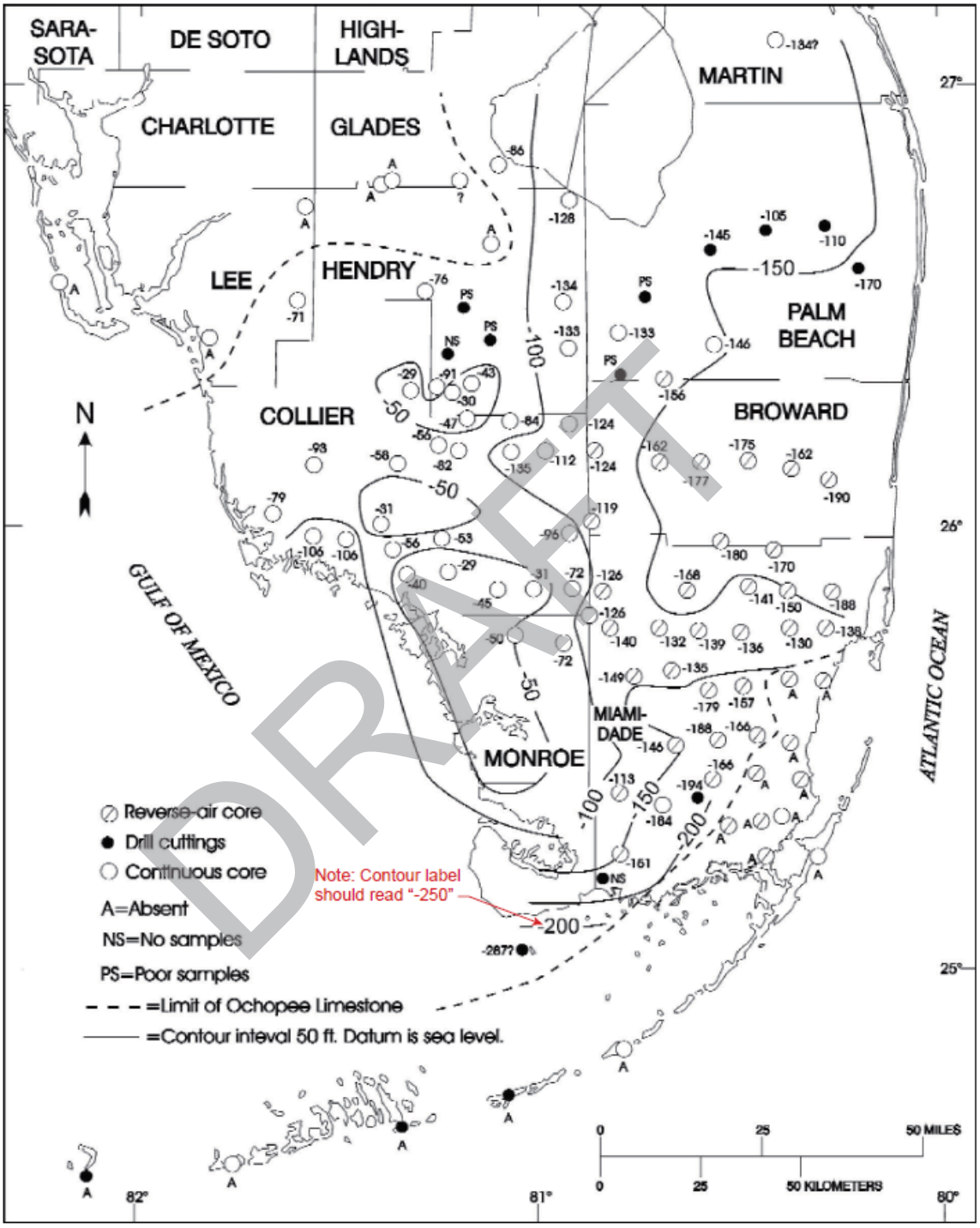

Figure 9. Figure 8 from Cunningham (2001); Structure contour map of the limestone within the Pliocene Tamiami formation.

This response is PLANT SPECIFIC

References:

Cunningham, K. J., Bukry, D., Sato, T., Barron, J. A., Guertin, L. A., Reese, R. S., 2001, Sequence stratigraphy of a south Florida carbonate ramp and bounding siliciclastics (Late Miocene-Pliocene); Florida Geological Survey Special Publication 49, p. 35-66.

Cunningham, K. J., Locker, S. D., Hine, A. C., Bukry, D., Barron, J. A., Guertin, L. A., 2003, Interplay of late Cenozoic siliciclastic supply and carbonate response on the southeast Florida platform: Journal of Sedimentary Research, v. 73, p. 31-46.

Florida Geological Survey (FGS) website, Lithologic database, http://publicfiles.dep.state.fl.us/FGS/WEB/lithologic/sfwmd2.zip, accessed 5/2/2012.

Guertin, L. A., Missimer, T. M., McNeill, D. F., 2000, Hiatal duration of correlative sequence boundaries from Oligocene-Pliocene mixed carbonate/siliciclastic sediments of the south Florida Platform: Sedimentary Geology, v. 134, p. 1-26.

Hine A. C., Suthard, B. C., Locker, S. D., Cunningham, K. J., Duncan, D. S., Evans, M., Morton, R. A., 2009, Karst sub-basins and their relationship to the transport of Tertiary siliciclastic sediments on the Florida Platform: International Association of Sedimentologists Special Publication: v. 41, p. 179-197.

McNeil, D. F., Cunningham, K. J., Guertin, L. A., Anselmetti, F. S., 2004, Depositional themese of mixed carbonate-siliciclastics in the south Florida neogene: Application to ancient deposits, in Integration of outcrop and modern analogs in reservoir modeling: AAPG Memoir 80, p. 23-43.

Miller, J. A., 1986, Hydrogeologic framework of the Floridan Aquifer system in Florida and parts of Georgia, Alabama, and South Carolina: USGS Professional Paper 1403-B, 91 p.

Missimer, T. M., 2001, Siliciclastic facies belt formation and the Late Oligocene to Middle Miocene partial drowning of the southern Florida platform, Gulf Coast Association of Geological Societies Transacations, v. LI, p. 229-238.

Scott, T., 2001, Geologic map of the state of Florida, Florida Geological Survey Open File Report 80.

Warzeski, E. R., Cunningham, K. J., Ginsburg, R. N., Anderson, J. B., Ding, Z. D., 1996, A Neogene mixed siliciclastic and carbonate foundation for the Quaternary carbonate shelf, Florida Keys, Journal of Sedimentary Research, V. 66, p. 788-800.

ASSOCIATED COLA REVISIONS:

A paragraph regarding the queried fault will be added to the FSAR Subsection 2.5.1.1.1.3.2.1. in a future COLA revision.

Queried Fault from Reference 373

Cunningham et al. (1998) (Reference 373) postulate that a fault or paleotopography could be responsible for elevation variations in the Arcadia formation in southwestern Florida (Figure 2.5.1-229). The queried structure is between 50 and 60 kilometers long (30 - 36 miles) (Figure 2.5.1-229) and at its nearest approach, the eastern end of the queried fault is approximately 41 kilometers (25 miles) west of the Turkey Point Units 6 & 7 site.

Figure 2.5.1-234 shows a cross-section across southern Florida that was developed with data from eight wells in southern Florida, with variable horizontal scale between pairs of wells, and thus with variable vertical exaggeration. Between the southernmost two wells, Cunningham et al. (1998) postulate the existence of a fault that cuts up through Avon Park Formation,

Suwannee Limestone, and Oligocene-Miocene-age Arcadia Formation, and potentially places the Arcadia Formation in fault contact with the lower portion of the overlying Miocene-Pliocene Long Key Formation. Alternatively, the Long Key Formation may be interpreted as deposited across a paleoscarp. Reference 373 labels the postulated fault on this cross-section with two question marks, indicating the speculative nature of this fault.

In cross section the postulated fault cuts units as young as the Miocene Arcadia formation, and although the Miocene to Pliocene Long Key Formation and the Pleistocene Key Largo are depicted as unfaulted, they have thickness and elevation differences across the structure (Figure 2.5.1-234). Higher up-section above the queried fault tip, Cunningham et al.'s (1998) cross-section shows marine carbonate stringers that could be interpreted as deformed by slip on the underlying fault. Alternatively, these marine carbonate stringers could represent deposition draped across a paleoscarp and thus could post-date slip on the underlying postulated fault.

Although the postulated fault in Figure 2.5.1-234 would not represent a Quaternary faulting hazard for the site if it existed, in detail the thickness and stratigraphic variations may instead be related to paleotopography. Indeed, the top of the Arcadia Formation is known to be an erosional unconformity with significant paleotopographic variation. For example, "A distinct regional unconformity and subaerial exposure surface at the top of the Arcadia Formation separates the Long Key and Arcadia Formations" (Reference 393). A cross-section presented by Reference 393 depicts 90 meters of relief on the top of the Arcadia Formation surface in southern Florida, while the thickness of the Arcadia Formation varies from 200 meters in the central portion of the Florida peninsula to between 0 and 20 meters farther east (Reference 394). A study in southern Florida determined that intensification of marine currents increased the erosion of marine carbonates and led to a significant time hiatus (more than 4 m.y.) following deposition of the Arcadia Formation (Reference 934) and the influence of Arcadia Formation paleotopography on highs in subsequent carbonate and clastic deposition in southernmost Florida has been recognized (Reference 395).

On Key Largo, relief on the top of the Arcadia Formation as large as 40 meters was found between borings only a few kilometers apart (Reference 393). Futhermore, in other cross sections presented by Reference 2.5.1-273, the elevation of the top of the Arcadia Formation varies by approximately 100 meters between wells W-3174 and W-17086 (88 km apart), by 50 meters between wells W-17156 and W12554 (56 km apart), and by 25 m between wells W-3011 and W-17157 (2 km apart), all interpreted without faulting. The slope required to achieve this latter elevation variation, 0.7 degrees, is actually greater than the slope required to achieve the elevation variation observed in the Arcadia Formation between the Everglades Park and Gulf Oil wells, where the queried fault is depicted in Figure 2.5.1-234 (approximately 100 meters over 18 kilometers of distance, or a 0.3 degree slope). Numerous other examples exist throughout southern Florida of steeper paleotopographic slopes on the top of the Arcadia Formation that are not associated with faulting. In addition, the down-to-the-south separation depicted on the postulated fault in Figure 1 is consistent with, and may, in part, be attributed to the regional southward dip of the strata towards the South Florida Basin in the area (e.g., Reference 389; Reference 377).

The karst-influenced paleotopography of the Arcadia Formation is detailed in Reference 936. While using borings at a much finer spacing than Cunningham study, the Hine study documents karst sub-basins with as much as 100 meters of relief over distances of kilometers to tens of

kilometers on the top of the Arcadia Formation in west-central Florida. They attribute this relief to a mid to late Miocene sea-level lowstand that caused dissolution in the deeper carbonates, such as the Arcadia Formation, and formed paleotopographic depressions and non-tectonic deformation in the Arcadia Formation (Reference 936).

Alternative interpretations of well data in southern Florida, often including the three wells closest to the postulated fault, provide evidence for unfaulted Eocene to Pliocene stratigraphy in the same location (e.g., References 393, 389, 934, 935). For example, Reference 934 provides a stratigraphic correlation diagram across the projection of the queried fault from Cunningham et al. (1998) and interprets no faulting. This diagram also displays similar relief between boreholes on the top of the Arcadia to the north. Likewise, the regional north-south-oriented cross-section shown in Figure 2.5.1-233 intersects the projection of the queried fault and does not indicate faulting in the area.

As shown in Figure 2.5.1-351, there are three wells adjacent to the queried structure: Gulf Oil W-3510 south of the postulated fault and W-1115 and W-2404 north of it. The Gulf Oil well W-3510 appears to control the set of structure contours used to delineate the area of faulting (Figures 2.5.1-234 and 351). Yet, other published contour maps of the same well data use dashed contours and question marks to indicate uncertainty in contouring such sparse data in the Florida Bay area (Reference 393). A later publication (Reference 935) also provides interpretations of unfaulted Miocene to Pliocene stratigraphy in the same location as the postulated fault from Reference 273.

In summary, numerous other sources using similar well data indicate unfaulted strata that gently dips to the south in this location, reflecting the influence of the South Florida Basin (e.g., Reference 393, 389, 396, 827). The fault postulated by Reference 273 has not been documented in any subsequent investigations and numerous examples of paleotopographic variation in the top of the Arcadia support a non-fault-related origin for the stratigraphic variations seen in Figure 2.5.1-234.

The following figure will be revised in a future COLA revision:

Figure 2.5.1-229 Regional Tectonic Features

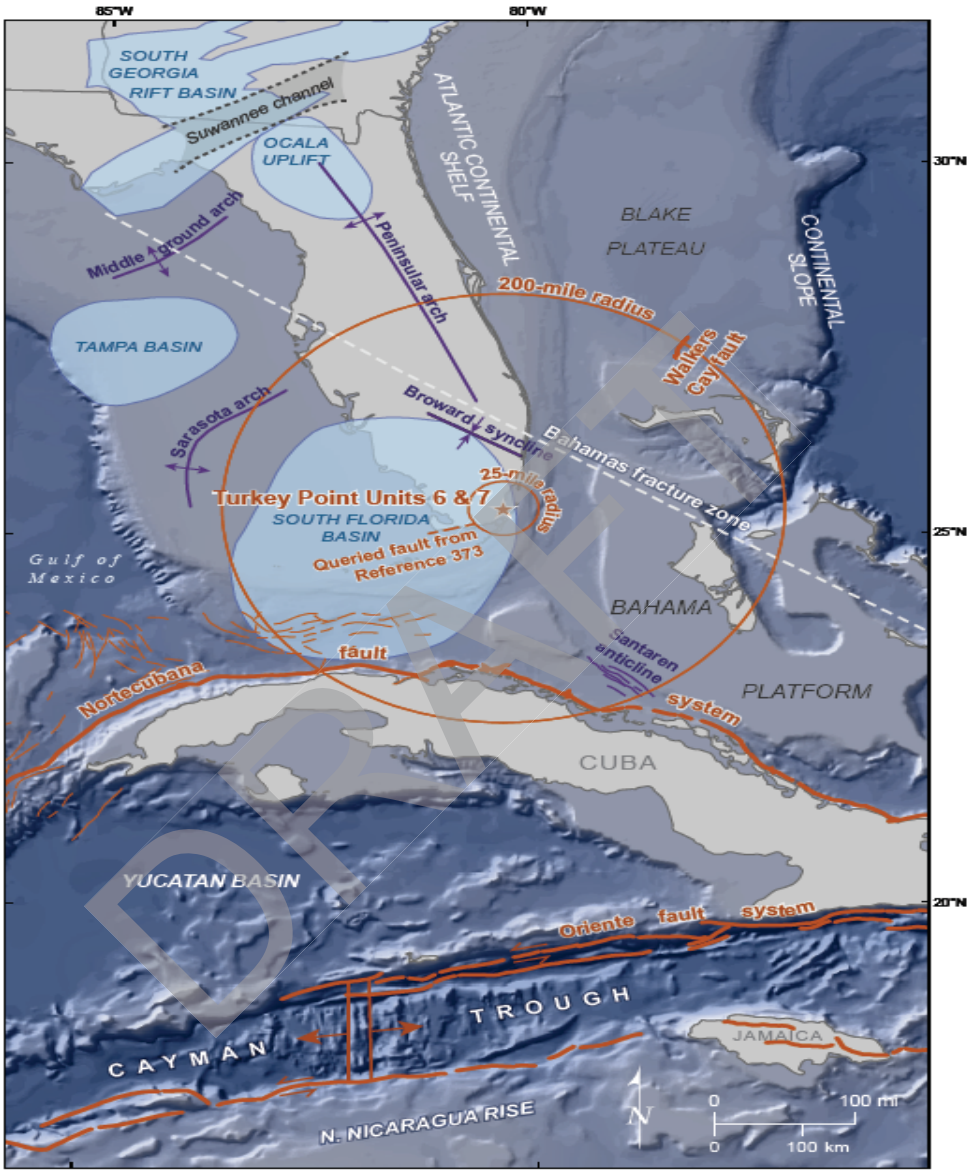

Sources: References 822, 482, 823, 457, 212, and 421

The following new figure will be included in FSAR Subsection 2.5.1 in a future COLA revision:

Figure 2.5.1-351 Structure Contour Map of the Top of the Oligiocene-Miocene Arcadia Formation

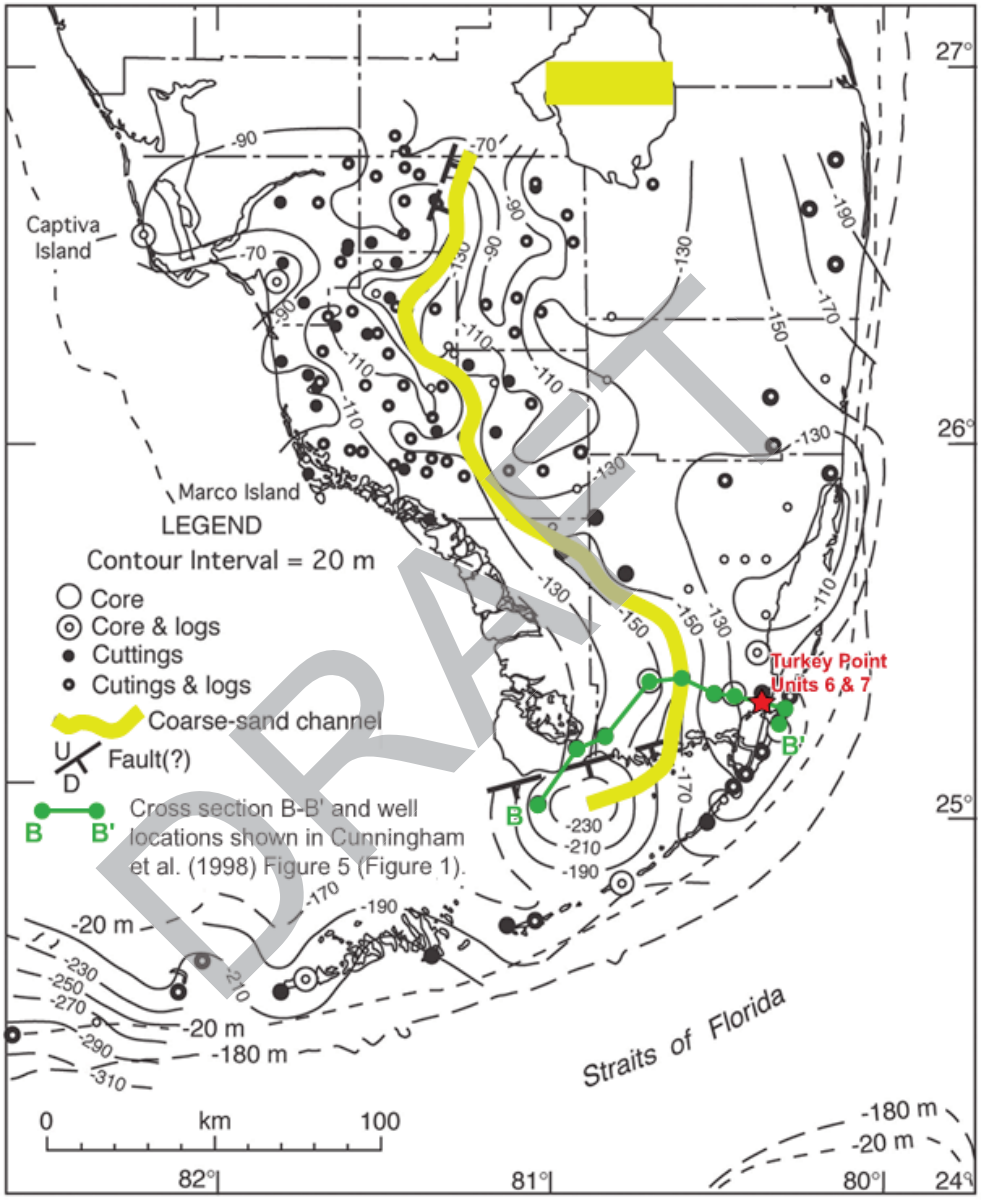

The following references will be included in FSAR Subsection 2.5.1.3 in a future COLA revision:

934. Guertin, L. A., Missimer, T. M., McNeill, D. F., 2000, Hiatal duration of correlative sequence boundaries from Oligocene-Pliocene mixed carbonate/siliciclastic sediments of the south Florida Platform: Sedimentary Geology, v. 134, p. 1-26.

935. Cunningham, K. J., Bukry, D., Sato, T., Barron, J. A., Guertin, L. A., Reese, R. S., 2001, Sequence stratigraphy of a south Florida carbonate ramp and bounding siliciclastics (Late Miocene-Pliocene); Florida Geological Survey Special Publication 49, p. 35-66.

936. Hine A. C., Suthard, B. C., Locker, S. D., Cunningham, K. J., Duncan, D. S., Evans, M., Morton, R. A., 2009, Karst sub-basins and their relationship to the transport of Tertiary siliciclastic sediments on the Florida Platform: International Association of Sedimentologists Special Publication: v. 41, p. 179-197.

ASSOCIATED ENCLOSURES:

None

NRC RAI Letter No. PTN-RAI-LTR-041

SRP Section: 02.05.01 - Basic Geologic and Seismic Information

QUESTIONS from Geosciences and Geotechnical Engineering Branch 2 (RGS2)

NRC RAI Number: 02.05.01-22 (eRAI 6024)

FSAR Section 2.5.1.1.1.2.3, the "Stratigraphy of Cuba" passage, states that "Late Miocene to Pliocene deposits are poorly developed and Pleistocene rocks include shelf and coastal carbonates that in places have been uplifted into terraces (Reference 383)". The staff notes that this implies Pleistocene tectonic uplift. The staff further notes that Agassiz (1894)[1] described the extensive marine terraces along the northern coast of Cuba and very young elevated patch reef corals in growth position, forming the lowest terraces. In addition, a suite of Quaternary terraces along the northern edge of Cuba is clearly depicted in available 1:500,000 scale geologic maps of the region.

In order for the staff to assess the tectonic and structural features within the site region and in accordance with 10 CFR 100.23, please address the following:

a) Explain the tectonic context of these uplifted terraces in light of continued seismicity along the northern coast of Cuba.
b) Discuss the ages, lateral extents, morphologies, and origins of the terraces.
c) Discuss the implications of these terraces for assessments of active faulting in the Site Region.

[1]Agassiz, A., 1894, A reconnaissance of the Bahamas and elevated reefs of Cuba: Bulletin of the Museum of Comparative Zoology, v. 26, 203 p.

FPL RESPONSE:

The components of the response to RAI 02.05.01-22 (eRAI 6024) are not presented in the same sequential order as the RAI question components. FPL has addressed the RAI question to respond to parts b, a, then c in order to first discuss the geology (stratigraphy), geomorphology, and the origin of the marine terraces followed by a discussion of the marine terraces in the context of seismicity and active faulting in the site region. FPL believes that by answering the questions in this manner, it will provide the NRC staff the context needed for staff to assess the tectonic and structural features within the site region.

b) Discuss the ages, lateral extents, morphologies, and origins of the terraces.

Along Cuba's north coast within the site region, the marine terraces that dip gently seaward (to the north) consist primarily of Miocene through Pleistocene age limestones (Reference 12 and Reference 13) and extend laterally along the north coast (FSAR 2.5.1 Reference 848) except where rivers have eroded gaps in the terraces (Reference 15). The terraces are wide with gentle slopes (as compared to those in southeastern Cuba), the karst processes (i.e., the formation of caves and caverns and sinkholes) are more pronounced, and notches (cuts along the base of a sea cliff near the high water mark that form by undercutting the sea cliff due to wave erosion and/or chemical solution) are pronounced (Reference 10). The Miocene rocks on which the marine terrace deposits formed are divided into the Cojimar Formation marls and the Güines Formation carbonates (chalks,

argillaceous bioclastic limestones, and reef limestones) that outcrop from Havana to Matanzas. The Cojimar Formation marls represent a middle Miocene deep open shelf that is overlain unconformably by the Güines Formation. The Güines Formation represents a carbonate platform that covered almost the entire Greater Antilles from the second half of the middle Miocene up to the late Miocene. Late Miocene-Pliocene deposits are only locally developed at the Morro Castle of Havana (the Morro limestones) and near Matanzas City at El Abra de Yumurí (El Abra Formation). The El Abra Formation is a fluvio-marine unit. Pleistocene carbonates of the Jaimanitas Formation (coral reef limestones and calcarenites) are exposed along the coastal plain of Havana and Matanzas (FSAR 2.5.1 Reference 383 and Reference 8) and along much of the north coast of Cuba (Reference 14).

Terraces in Cuba near Matanzas are classified as erosional, depositional/cumulative, and constructional (References 9 and 12). Erosional terraces on Cuba's northern coastline are located east of Boca de Juruco, province of Havana and in the vicinity of the Bay of Matanzas (Reference 12). Cumulative terraces are described as: (1) having a sandy beach with an inner edge of 3.3 to 4.9 feet (1 to 1.5 meters) above sea level and (2) storm bank with heights of 6.6 to 9.8 feet (2 to 3 meters) above sea level. Cumulative terraces occur on the northern coastline of Cuba, east of Havana. Constructional coral reef terraces are located on the north coast west of Havana to Mariel and the suburbs of Havana and Santa Fe Jaimanitas (References 9 and 12).

Four marine terraces near Havana occur at elevations 200, 100, 10-15 and 4-5 feet (61, 31, 3.1-4.6 and 1.2-1.5 meters) above mean sea level (FSAR 2.5.1 Reference 383; References 6, 7 and 15). Near Matanzas, six terraces have been observed at elevations 400, 300, 200, 140, 30, and 5-6 feet (122, 91, 61, 43, 9, and 1.5-1.8 meters) above sea level (References 6, 7 and 15). At Matanzas Bay, Ducloz (Reference 4), Shanzer et al., (Reference 12) and Penalver Hernandez et al., (Reference 10) observed four terraces at the following approximate elevations 82-167 feet (25-51 meters) (Rayonera), 49-108 feet (15-33 meters) (Yucayo), +/- 52 feet (+/-16 meters) (Puerto) and +/- 26 feet (+/-8 meters) (Terraza de Seboruco) (Table1).

The Rayonera terrace is strongly karstic. The presence of sinkholes and caves indicate that the outer edge of the terrace has a height of 128 feet (39 meters) whereas the inner edge is around 167 feet (51 meters) giving this surface a topographic slope of about 3 to 4 degrees towards the coast. The rocks of this terrace are Pliocene-Pleistocene in age. As noted by its name, the Yucayo terrace is "narrow". It has an average height of 98 feet (30 meters) near the Bay of Matanzas. The terrace is cut off from the sea by a vertical cliff that is approximately 20 to 46 feet (6 to 14 meters) in height. Sea caves are present and are indicative of coastal erosion. The Pliocene-Pleistocene rocks of this terrace are algal conchiferas with hard, massive, and recrystallized limestone reefs. The Pliocene-Pleistocene Puerto terrace is similar to the Yucayo and Rayonera terraces. All three are characterized by the development of karst, sinkholes and a very sharp weathering surface known "diente de perros" (dog's teeth) (References 4 and 10).

The Terraza de Seboruco, the youngest of these terraces is located west of Matanzas Bay. It rises +2 to 3 meters (+6.6 to 9.8 feet) above mean sea level with paleolagoonal facies extending inland 1 or more kilometers. Near Havana and Matanzas, the elevation of the Terraza de Seboruco ranges from +2 to +3 meters (6.6 to 9.8 feet) above mean sea level to

+4 to 5 meters (13 to 16 feet) above mean sea level respectively. The terrace is described as porous or cavernous fossilized limestone from the Pleistocene Jaimanitas Formation with a weathering surface of diente de perros (References 4 and 14).

The terraces and sea cliffs form a stair-step sequence, which suggests that reef deposition was followed by high sea level stands that cut the bench-like features in the sea cliffs (Reference 1). Several alternate processes can explain or partially explain the stair-step morphology and bench-like features that were described by Agassiz (Reference 1), Spencer (Reference 13) and Ducloz (Reference 4). The alternate hypotheses for what might have contributed to terrace formation as discussed in FSAR Subsections are eustatic changes in sea level (FSAR Subsection 2.5.1.1.1.1.1.1), changes in ocean circulation pattern (FSAR Subsection 2.5.1.1), rise and fall in sea level as a direct result of melting and formation of the continental glaciers (FSAR Subsection 2.5.1.1.1.1.1.1), and tectonic activity (FSAR Subsections 2.5.1 [Overview of Tectonic Evolution Cretaceous to Tertiary, Caribbean-North American Plate Convergence, and Tertiary Transfer of Cuba to the North American Plate] and 2.5.1.3.3).

Uranium-thorium (U-Th) dates were obtained on corals (two very large *Montastrea* sp. and one *Acropora* palmate) from the Terraza de Seboruco at the Cantera Playa Baracoa quarry and in the Santa Cruz del Norte canal. When corrected from the initial Uranium age dates, the ages of the samples correspond to the Marine Isotope Stage 5e sea level high stand at approximately 120–130 ka (Reference 14). Toscano et al. (Reference 14) observe that similar age terraces throughout stable portions of the Caribbean area are at similar elevations, which is evidence for the absence of active uplift near Matanzas in the past 120–130 ka. Therefore, based on the U-Th dates, the Terraza de Seboruco is correlative to the Cockburntown reef (Bahamas) (Reference 3), Barbados III (Barbados) (Reference 5), and Key Largo Limestone (Florida) (References 2 and 11).

a) Explain the tectonic context of these uplifted terraces in light of continued seismicity along the northern coast of Cuba.

Elevated marine terraces were identified along the northern coast of Cuba as early as the late 19th century (Reference 1). Recent studies of the marine terraces along the north coast of Cuba, especially for the stretch between Matanzas and Havana, are summarized below. As noted above, Ducloz (Reference 4) provides a description of the Quaternary deposits and surfaces in the Matanzas region, including the Pleistocene-age Terraza de Seboruco surface west of Matanzas Bay. Ducloz (Reference 4) suggests that the elevated marine terraces along Cuba's north coast likely formed as the result of both fluctuations in sea level and epeirogenic uplift (Table 1). Ducloz (Reference 4) suggests that reactivation of a regional scale anticline may be partly responsible for formation of the terrace surfaces near Matanzas.

Similarly, Shanzer et al. (Reference 12) identify three Pleistocene-age marine terraces in the Matanzas-Havana region. Shanzer et al (Reference 12) correlate to segments of the Pleistocene-age Terraza de Seboruco between Matanzas and Havana and suggest that this terrace is approximately 1.5 to 3 meters (4.9 to 9.8 feet) lower at Havana than at Matanzas. Shanzer et al (Reference 12) do not consider erosion of the terrace surface to explain the difference in elevation between Havana and Matanzas. Shanzer et al. (Reference 12) postulate that this difference in elevation may be the result of differential

tectonic uplift, but they do not suggest what structure or structures may be responsible for this postulated tectonic uplift.

Toscano et al. (Reference 12) also observe that the Terraza de Seboruco (ages discussed above) in the Matanzas area is just a few meters above mean sea level, similar to the elevation of other Substage 5e reef deposits throughout stable portions of the Caribbean and therefore can be explained solely by changes in sea level. Toscano et al. (Reference 14) conclude, “no obvious tectonic uplift is indicated for this time frame along the northern margin of Cuba” (p. 137).

Pedoja et al. (Reference 9) investigate late Quaternary coastlines worldwide and observe minor uplift relative to sea level of approximately 0.2 millimeters per year, even along passive margins, outpacing eustatic sea level decreases by a factor of four. Pedoja et al. (Reference 9) suggest that the decreasing number of subduction zones since the Late Cretaceous, coupled with relatively constant ridge length, has resulted in an increase in the average magnitude of compressive stress in the lithosphere. They argue that this average increase in compressive stress has produced low rates of uplift, even along passive margins as observed in their widespread measurements of uplifted continental margins. The measurements specific to Cuba suggest that the Substage 5e terrace in the Matanzas area (i.e., the Terraza de Seboruco) has been uplifted at an average rate that ranges from approximately 0.00 to 0.04 millimeter per year over the last approximately 122 ka (Reference 9).

The Turkey Point Units 6 & 7 phase 2 earthquake catalog indicates sparse minor- to light-magnitude seismicity along Cuba’s north coast between Havana and Matanzas (Figures 1A and 1B in FPL’s supplemental response to RAI 02.05.01-21). It is possible that these earthquakes occurred on faults partially responsible for uplift of the marine terraces along Cuba’s north coast in the site region. However, the association of the uplift of these terraces and earthquakes with individual faults in northern Cuba is uncertain. Based on the Turkey Point Units 6 & 7 phase 2 earthquake catalog, earthquakes do not appear to be aligned along faults in the Matanzas-Havana region. In addition, there are no known focal mechanisms available for these earthquakes that would help to constrain the causative fault or faults nor is there sufficient data to correlate uplift of marine terraces with these individual faults in northern Cuba.

c) Discuss the implications of these terraces for assessments of active faulting in the Site Region.

It is possible that the elevations above modern sea level of marine terraces along Cuba’s north coast in the site region are partially the result of tectonic uplift (References 4 and 12). Based on extensive literature review performed for this project, to FPL’s knowledge, the Terraza de Seboruco is the only terrace in northern Cuba for which radiometric age control is available. There is not sufficient data on this or other marine terraces in northern Cuba to assess the implications for active faulting. As described in this response (parts a and b), Toscano et al.’s (Reference 14) U-Th analyses of corals collected from the Terraza de Seboruco indicates that tectonic uplift is not required to explain the present elevation of this Substage 5e terrace. Instead, they conclude that the elevation of this terrace surface is consistent with other Substage 5e terraces in other tectonically stable regions of the Caribbean and that global fluctuations in sea level, not tectonic uplift, are responsible for

the Terraza de Seboruco's present elevation above modern sea level. Likewise, Pedoja et al.'s (Reference 9) global study suggests that the elevation of the Terraza de Seboruco is consistent with the elevations of other Substage 5e terraces in tectonically stable regions worldwide.

Based on recent studies by Toscano et al. (Reference 14) and Pedoja et al. (Reference 9), active faulting is not required to explain the elevation of the Terraza de Seboruco along Cuba's north coast in the site region. However, observations of the Terraza de Seboruco cannot necessarily be used to preclude possible strike-slip faulting in the site region. As shown by the Turkey Point Units 6 & 7 phase 2 earthquake catalog, only sparse minor- to light-magnitude seismicity is observed along Cuba's northern coast between Havana and Matanzas. It is possible that at least some of these earthquakes occurred on the faults mapped in the region. However, in the absence of well-located hypocenters and focal mechanisms, these earthquakes cannot be definitively attributed to a particular fault or faults.

.

Table 1 Marine Terraces in the Matanzas Area of Northern Cuba

Marine Terrace (Reference 4)	Elevation of Marine Terrace (Reference 4)	Geologic Stratum (References 4 and 10)	Depositional Environment (Reference 4)	Possible Geologic Age (Reference 4)	Possible Geologic Age (Reference 10)
			Start of emergence	Start of the Upper Miocene	
			Erosion Cycle (No. 1)	Upper Miocene	
			Uplift and buckling (env. 60 m)	Pliocene (?)	
			Erosion Cycle (No. 2)		
			Uplift (env. 80 m)	Pliocene	
			Erosion Cycle (No. 3)		
			Uplift and folding (10 and 45 m)		
La Rayonera	25 and 51 m		Erosion Cycle (No. 4)		Pliocene-Pleistocene
			Uplift and folding (15 and 25 m)		
Yucayo	15 and 33 m		Erosion epicycle (No. 1)	Pliocene (?)	Pliocene-Pleistocene
			Drop in sea level: uplift, very light folding (10 m)	Pliocene (?)	
Puerto	16 m		Erosion epicycle (No. 2)	Start of the Illinoian Glaciation	
			Drop in sea level (11 and 13 m)		
submarine terrace	No. 1 (-1 m)		Erosion epicycle (No. 3)		
			Drop in sea level (1 m)		
submarine terrace	No. 2 (-2 and -6 m)		Erosion epicycle (No. 4)		
			Drop in sea level (env. 130 m)	Illinoian Glaciation Maximum	
Continental Shelf terrace			Erosion epicycle (No. 5)		
			Rise in eustatic sea level (+11 m)	Sangamon Interglacial	
		Jaimanitas Formation (Terraza de Seboruco), Rosario Terrace (continental alluvial terrace)	Formation of fringing reefs on uplifted alluvium deposits		Pleistocene
Limits of the Terraza de Seboruco	+/- 8 m		Drop in sea level (env. 12 m)	Start of the Wisconsinan Glaciation	
submarine terrace	No. 3 (-10 and -17 m)		Erosion epicycle (No. 6)		
			Drop in sea level (env. 10 m)		
submarine terrace	No. 4 (-20 and -55 m)		Erosion epicycle(No. 7)		
			Drop in sea level (env. 110 m)	Wisconsinan Glaciation Maximum	
Limit of the Restart of the Continental Plate			Erosion epicycle (No. 8)		
			Eustatic rise to present sea level	FlandrianTransgression	
		Recent alluvium	Induation of river valleys		

This response is PLANT SPECIFIC

References:

1. Agassiz, A., A reconnaissance of the Bahamas and elevated reefs of Cuba: Bulletin of the Museum of Comparative Zoology, v. 26, p. 203, 1894.
2. Broecker, W.S. and Thurber, D. L., Uranium-series dating of coral and oolites from Bahaman and Florida Key limestones: Science, vol. 149, pp. 58-60, 1965.
3. Chen, J. H., Curran, H. A., White, B., Wasserburg, G. J., Precise chronology of the last interglacial period: 234U-230 Th data from fossil coral reefs in the Bahamas: Geological Society of America Bulletin, vol., 103, pp. 82-97, 1991.
4. Ducloz, C., Etude geomorphologique de la region de Matanzas, Cuba avec une contribution a l'etude des depots quaternaires de la zone Habana-Matanzas, Archives des Sciences, Societe de Physique et d'Histoire Naturelle de Geneve, Imprimerie Kundig, 402 pp, 1963.
5. Gallup, C. D., Edwards, R. L., and Johnson, R. G., The timing of high sea levels over the past 200,000 years: Science, vol. 263, pp. 796-800, 1994.
6. Hayes, C.W., Vaughan, T.W., and Spencer, A.C., A Geological Reconnoissance [sp] of Cuba, pp. 18-20, 1901.
7. Hill, R.T., Notes on the Geology of the Island of Cuba, Based Upon a Reconnoissance [sp] Made for Alexander Agassiz, Bulletin of the Museum of Comparative Zoology, v. XVI, no. 15, pp. 264-274, 1895.
8. Iturralde-Vinent, M.A., Linked Earth Systems Field Guide Sedimentary Geology of Western Cuba, The 1st SEPM Congress on Sedimentary Geology August 13-16, 1995, St. Pete Beach Florida, 1995.
9. Pedoja, K., Husson, L., Regard, V., Cobbold, P.R., Ostanciaux, E., Johnson, M.E., Kershaw, S., Saillard, M., Martinod, J., Furgerot, L., Weill, P., and Delcaullau, B., Relative sea-level fall since the last interglacial state: Are coasts uplifting worldwide?, Earth Science Reviews, v. 108, p. 1-15, 2011.
10. Penalver Hernandez, L, L., Castellanos Abella, E., Perez Aragon, R. O., and Rivada Suarez, R., Las Terrazas Marinas de Cuba y Su Correlacion Con Algunas Del Area Circumcaribe, Memorias Geomin, V Congreso de Geologia y Mineria, 24-28 De Marzo, La Habana, pp. 10, 2003.
11. Osmond, J. K., Carpenter, J.R., and Windom, H.L., 230 Th/234 U age of Pleistocene corals and oolites of Florida: Journal of Geophysical Research, vol. 70, pp. 1843-1847, 1965.
12. Shanzer, E.V., Petrov, O.M., and Franco, G., Sobre las formaciones costeras del Holoceno en Cuba, las terrazas Pleistocenicas de la region Habana-Matanzas y los sedimentos vinculados a ellas, Serie Geologica no. 21, Acadamia de Ciencias de Cuba, Instituto de Geologia y Paleontologia, p. 1-26, 1975.

13. Spencer, J.W., Geographical Evolution of Cuba, Bulletin of the Geological Society of America, v. 7, pp. 67-94, 1895.

14. Toscano, M.A., Rodriguez, E., and Lundberg, J., Geologic investigation of the late Pleistocene Jaimanitas formation: science and society in Castro's Cuba, Proceedings of the 9th Symposium on the Geology of the Bahamas and Other Carbonate Regions, Bahamian Field Station, Ltd., San Salvador, Bahamas. p. 125-142, 1999.

15. Vaughan, T.W., and Spencer, A., The Geography of Cuba, Bulletin of the American Geographical Society, v. 34, no. 2, pp. 105-116, 1902.

ASSOCIATED COLA REVISIONS:

The following text in FSAR Subsection 2.5.1.1.1.2.3, Stratigraphy of Cuba, will be revised in a future revision of the COLA.

After the last paragraph of this subsection:

The Eocene-Oligocene contact is at a depth of approximately 4500 feet (1370 meters). The Oligocene unit consists of up to 600 feet (183 meters) of deep-water chalk and limestone that grades laterally into an arenaceous and shaly limestone deposited in marine water of intermediate depth. This is overlain by 400 to 1000 feet (120 to 300 meters) of Miocene sediments consisting of deep-water marl, siltstone, and shaly limestone that grade into arenaceous and calcareous sediments with intercalated, fossiliferous sandy limestone deposited in a neritic environment (Reference 382). Late Tertiary deposits occur in the northern coastal area and dip gently toward the north. ~~Miocene rocks are divided into marl and carbonate units. Miocene and younger deposits are described as horizontal or only slightly tilted (Reference 440). Late Miocene to Pliocene deposits are poorly developed and Pleistocene rocks include shelf and coastal carbonates that in places have been uplifted into terraces (Reference 383).~~

Along Cuba's north coast within the site region, the marine terraces that dip gently seaward (to the north) consist primarily of Miocene through Pleistocene age limestones (References 924 and 923) and extend laterally along the north coast (Reference 848) except where rivers have eroded gaps in the terraces (Reference 926). The terraces are wide, with gentle slopes, the karst processes are more pronounced (i.e., the formation of caves and caverns and sinkholes), and notches (a cut along the base of a sea cliff near the high water mark that forms by undercutting the sea cliff due to wave erosion and/or chemical solution) are pronounced (Reference 921). The Miocene rocks that the marine terrace deposits formed are divided into the Cojimar Formation marls and the Güines Formation carbonates (chalks, argillaceous bioclastic limestones, and reef limestones) that outcrop from Havana to Matanzas. The Cojimar Formation marls represent a middle Miocene deep open shelf that is overlain unconformably by the Güines Formation. The Güines Formation represents a carbonate platform that covered almost the entire Greater Antilles from the second half of the middle Miocene up to the late Miocene. Late Miocene-Pliocene deposits are only locally developed at the Morro Castle of Havana (the Morro limestones) and near Matanzas City at El Abra de Yumurí (El Abra Formation). The El Abra Formation is a fluvio-marine unit. Pleistocene carbonates of

the Jaimanitas Formation (coral reef limestones and calcarenites) are exposed along the coastal plain of Havana and Matanzas (References 383 and 919) and along much of the north coast of Cuba (Reference 925).

Terraces in Cuba near Matanzas are classified as erosional, depositional/cumulative and constructional (References 923 and 920). Erosional terraces on Cuba's northern coastline are located east of Boca de Juruco, province of Havana and in the vicinity of the Bay of Matanzas (Reference 923). Cumulative terraces are described as: (a) having a sandy beach with an inner edge of 3.3 to 4.9 feet (1 to 1.5 meters) above sea level, and (b) storm bank with heights of 6.6 to 9.8 feet (2 to 3 meters) above sea level. Cumulative terraces occur on the northern coastline of Cuba, east of Havana. Constructional coral reef terraces are located on the north coast west of Havana to Mariel and the suburbs of Havana and Santa Fe Jaimanitas (References 923 and 920).

Four marine terraces near Havana occur at elevations 200, 100, 10-15 and 4-5 feet (61, 31, 3.1-4.6 and 1.2-1.5 meters) above mean sea level (References 383, 918, 917, and 926). Near Matanzas six terraces have been observed at elevations 400, 300, 200, 140, 30, and 5-6 feet (122, 91, 61, 43, 9, and 1.5-1.8 meters) above sea level (References 918, 917, and 926). At Matanzas Bay, Ducloz (Reference 915), Shanzer et al., (Reference 923) and Penalver Hernandez et al., (Reference 921) observed four terraces at the following approximate elevations 82-167 feet (25-51 meters) (Rayonera), 49-108 feet (15-33 meters) (Yucayo), +/- 52 feet (+/-16 meters) (Puerto) and +/- 26 feet (+/-8 meters) (Terraza de Seboruco) (Table 2.5.1-208). The Rayonera terrace is strongly karstic. The presence of sinkholes and caves indicate that the outer edge of the terrace has a height of 128 feet (39 meters) whereas the inner edge is around 167 feet (51 meters) giving this surface a topographic slope of about 3 to 4 degrees towards the coast. The rocks of this terrace are Pliocene-Pleistocene in age. As noted by its name, the Yucayo terrace is "narrow". It has an average height of 98 feet (30 meters) near the Bay of Matanzas. The terrace is cut off from the sea by a vertical cliff that is approximately 20 to 46 feet (6 to 14 meters) in height. Sea caves are present and are indicative of coastal erosion. The Pliocene-Pleistocene rocks of this terrace are algal conchiferas, with hard, massive, and recrystallized limestone reefs. The Pliocene-Pleistocene Puerto terrace is similar to the Yucayo and Rayonera terraces. All three are characterized by the development of karst, sinkholes and a very sharp weathering surface known "diente de perros" (dog's teeth) (References 915 and 921). The Terraza de Seboruco , the youngest of these terraces is located west of Matanzas Bay. It rises just a few meters (+2 to 3 meters) (+6.6 to 9.8 feet) above mean sea level with paleo-lagoonal facies extending inland one or more kilometers. Near Havana and Matanzas, the elevation of the Terraza de Seboruco ranges from +2 to +3 meters (6.6 to 9.8 feet) above mean sea level to +4 to 5 meters (13 to 16 feet) above mean sea level respectively. The terrace is described as porous or cavernous fossilized limestone from the Pleistocene Jaimanitas Formation with a weathering surface of "diente de perros" (References 915 and 925).

The terraces and sea cliffs form a stair-step sequence, which suggests that reef deposition was followed by high sea level stands that cut the bench-like features in the sea cliffs (Reference 912). Several alternate processes can explain or partially

explain the stair-step morphology and bench-like features that were described by Agassiz (Reference 912), Spencer (Reference 924) and Ducloz (Reference 915). The alternate hypotheses for what might have contributed to terrace formation as discussed in FSAR Subsections are eustatic changes in sea level (FSAR Subsection 2.5.1.1.1.1.1.1), changes in ocean circulation pattern (FSAR Subsection 2.5.1.1), rise and fall in sea level as a direct result of melting and formation of the continental glaciers (FSAR Subsection 2.5.1.1.1.1.1.1), and tectonic activity (FSAR Subsections 2.5.1 [Overview of Tectonic Evolution Cretaceous to Tertiary, Caribbean-North American Plate Convergence, and Tertiary Transfer of Cuba to the North American Plate] and 2.5.1.3.3).

Uranium-thorium (U-Th) dates were obtained on corals (two very large *Montastrea* sp. and one *Acropora* palmate) from the Terraza de Seboruco at the Cantera Playa Baracoa quarry and in the Santa Cruz del Norte canal. When corrected from the initial Uranium age dates, the ages of the samples correspond to the Marine Isotope Stage 5e sea level high stand at approximately 120–130 ka (Reference 925). Toscano et al. (Reference 925) observe that similar age terraces throughout "stable" portions of the Caribbean area are at similar elevations, which is evidence for the absence of active uplift near Matanzas in the past 120-130 ka. Therefore, based on the U-Th dates, the Terraza de Seboruco is correlative to the Cockburntown reef (Bahamas) (Reference 914), Barbados III (Barbados) (Reference 916), and Key Largo Limestone (Florida) (References 913 and 922).

The following text in FSAR Subsection 2.5.1.1.1.3.2.4, Cuba, will be revised in a future revision of the COLA.

After the last paragraph of Structures of Cuba in this subsection:

Nonetheless, available geologic mapping (at 1:250,000 and 1:500,000 scales; References 846, 847, and 848) provides some information regarding the timing of activity for some of the regional structures and largely indicates that the Pleistocene and younger strata are undeformed throughout the island. This is consistent with geodetic data that indicate that less than 3 millimeters/year of deformation is occurring within Cuba relative to North America (References 502 and 503). The available data indicate that the Oriente fault system, located offshore just south of Cuba, should be characterized as a capable tectonic source. Aside from the Oriente fault, no clear evidence for Pleistocene or younger faulting is available for any of the other regional tectonic structures on Cuba, and none of these faults are adequately characterized with late Quaternary slip rate or recurrence of large earthquakes. The scales of available geologic mapping (1:250,000 and 1:500,000; References 846, 847, and 848) do not provide sufficient detail to adequately assess whether or not individual faults in Cuba can be classified as capable tectonic structures.

Additionally, elevated marine terraces were identified along the northern coast of Cuba as early as the late 19th century (Reference 912). Recent studies of the marine terraces along the north coast of Cuba, especially for the stretch between Matanzas and Havana, are summarized below. Subsection 2.5.1.1.1.2.3 provides a description of the Quaternary deposits and surfaces in the Matanzas region, including the Pleistocene-age Terraza de Seboruco surface west of Matanzas Bay. Ducloz (Reference 915) suggests that the elevated marine terraces along Cuba's north coast

likely formed as the result of both fluctuations in sea level and epeirogenic uplift (Table 2.5.1-208). Ducloz (Reference 915) suggests that reactivation of a regional scale anticline may be partly responsible for formation of the terrace surfaces near Matanzas.

Similarly, Shanzer et al. (Reference 923) identify three Pleistocene-age marine terraces in the Matanzas-Havana region. Shanzer et al. (Reference 923) correlate segments of the Pleistocene-age Terraza de Seboruco between Matanzas and Havana and suggest that this terrace is approximately 1.5 to 3 meters (4.9 to 9.8 feet) lower at Havana than at Matanzas. Shanzer et al. (Reference 923) do not consider erosion of the terrace surface to explain the difference in elevation between Havana and Matanzas. Shanzer et al. (Reference 923) postulate that this difference in elevation may be the result of differential tectonic uplift, but they do not suggest what structure or structures may be responsible for this postulated tectonic uplift.

Toscano et al. (Reference 925) also observe that the Terraza de Seboruco in the Matanzas area is just a few meters above mean sea level, similar to the elevation of other Substage 5e reef deposits throughout "stable" portions of the Caribbean, and therefore can be explained solely by changes in sea level. Toscano et al. (Reference 925) conclude, "no obvious tectonic uplift is indicated for this time frame along the northern margin of Cuba" (p. 137).

Pedoja et al. (Reference 920) investigate late Quaternary coastlines worldwide and observe minor uplift relative to sea level of approximately 0.2 millimeter per year, even along passive margins, outpacing eustatic sea level decreases by a factor of four. Pedoja et al. (Reference 920) suggest that the decreasing number of subduction zones since the Late Cretaceous, coupled with relatively constant ridge length, has resulted in an increase in the average magnitude of compressive stress in the lithosphere. They argue that this average increase in compressive stress has produced low rates of uplift even along passive margins, as observed in their widespread measurements of uplifted continental margins. The measurements specific to Cuba suggest that the Substage 5e terrace in the Matanzas area (i.e., the Terraza de Seboruco) has been uplifted at an average rate that ranges from approximately 0.00 to 0.04 millimeter per year over the last approximately 122 ka (Reference 920).

Seismicity of Cuba

Maps of instrumental and pre-instrumental epicenters for Cuba show that seismicity can be separated into two zones: (a) the very active plate boundary region, including the east Oriente fault zone along Cuba's southern coast, and (b) the remainder of the island away from the active plate boundary region, which exhibits low to moderate levels of seismic activity (Figures 2.5.1-267, 2.5.2-220, and 2.5.2-221). **Regarding zone b, along the north coast of Cuba between Havana and Matanzas, the Turkey Point Units 6 & 7 Phase 2 earthquake catalog indicates sparse minor- to light-magnitude seismicity. It is possible that these earthquakes occurred on faults partially responsible for uplift of the marine terraces along Cuba's north coast in the site region. However, the association of the uplift of these terraces and earthquakes with individual faults in northern Cuba is uncertain. Based on the Turkey Point Units 6 & 7 Phase 2**

earthquake catalog, earthquakes do not appear to be aligned along faults in the Matanzas-Havana region. In addition, there are no known focal mechanisms available for these earthquakes that would help to constrain the causative fault or faults nor is there sufficient data to correlate uplift of marine terraces with these individual faults in northern Cuba.

It is possible that the elevations above modern sea level of marine terraces along Cuba's north coast in the site region are partially the result of tectonic uplift (i.e., References 915 and 923). The Terraza de Seboruco is the only terrace in northern Cuba for which radiometric age control is available. There is not sufficient data on this or other marine terraces in northern Cuba to assess the implications for active faulting. As discussed in Subsection 2.5.1.1.1.2.3, Toscano et al.'s (Reference 925) U-Th analysis of corals collected from the Terraza de Seboruco indicates that tectonic uplift is not required to explain the present elevation of this Substage 5e terrace. Instead, they conclude that the elevation of this terrace surface is consistent with other Substage 5e terraces in other tectonically stable regions of the Caribbean and that global fluctuations in sea level, not tectonic uplift, are responsible for the Terraza de Seboruco's present elevation above modern sea level. Likewise, Pedoja et al.'s (Reference 920) global study suggests that the elevation of the Terraza de Seboruco is consistent with the elevations of other Substage 5e terraces in tectonically stable regions worldwide.

Based on studies by Toscano et al. (Reference 925) and Pedoja et al. (Reference 920), active faulting is not required to explain the elevation of the Terraza de Seboruco along Cuba's north coast in the site region. However, observations of the Terraza de Seboruco cannot necessarily be used to preclude possible strike-slip faulting in the site region. As shown by the Turkey Point Units 6 & 7 Phase 2 earthquake catalog, only sparse minor- to light-magnitude seismicity is observed along Cuba's northern coast between Havana and Matanzas. It is possible that at least some of these earthquakes occurred on the faults mapped in the region. However, in the absence of well-located hypocenters and focal mechanisms, these earthquakes cannot be definitively attributed to a particular fault or faults.

The east Oriente fault zone is an active plate boundary, with seismic activity concentrated on the Cabo Cruz Basin and the Santiago deformed belt. Focal mechanisms from the Cabo Cruz area show consistent east-northeast to west-southwest oriented normal faulting, indicative of an active pull-apart basin. In the Cabo Cruz Basin, all hypocenters are less then 30 kilometers (19 miles) deep. The Santiago deformed belt mechanisms show a combination of northwest-directed underthrusting and east-west left-lateral strike-slip, consistent with a bi-modal transpressive regime (Reference 504). In the Santiago deformed belt, thrust mechanisms occur between depths of 30 and 60 kilometers (19 and 37 miles), while the strike-slip mechanisms are shallower.

The following text in FSAR Subsection 2.5.1.3, References, will be revised in a future revision of the COLA.

912. Agassiz, A., A reconnaissance of the Bahamas and elevated reefs of Cuba: Bulletin of the Museum of Comparative Zoology, v. 26, p. 203, 1894.

913. Broecker, W.S. and Thurber, D. L., Uranium-series dating of coral and oolites from Bahaman and Florida Key limestones: Science, vol. 149, pp. 58-60, 1965.

914. Chen, J. H., Curran, H. A., White, B., Wasserburg, G. J., Precise chronology of the last interglacial period: 234U-230 Th data from fossil coral reefs in the Bahamas: Geological Society of America Bulletin, vol., 103, pp. 82-97, 1991.

915. Ducloz, C., Etude geomorphologique de la region de Matanzas, Cuba avec une contribution a l'etude des depots quaternaires de la zone Habana-Matanzas, Archives des Sciences, Societe de Physique et d'Histoire Naturelle de Geneve, Imprimerie Kundig, 402 pp, 1963.

916. Gallup, C. D., Edwards, R. L., and Johnson, R. G., The timing of high sea levels over the past 200,000 years: Science, vol. 263, pp. 796-800, 1994.

917. Hayes, C.W., Vaughan, T.W., and Spencer, A.C., A Geological Reconnoissance [sp] of Cuba, pp. 18-20, 1901.

918. Hill, R.T., Notes on the Geology of the Island of Cuba, Based Upon a Reconnoissance [sp] Made for Alexander Agassiz, Bulletin of the Museum of Comparative Zoology, v. XVI, no. 15, pp. 264-274, 1895.

919. Iturralde-Vinent, M.A., Linked Earth Systems Field Guide Sedimentary Geology of Western Cuba, The 1st SEPM Congress on Sedimentary Geology [sp] of Cuba, pp. 18-20, 1901.

920. Pedoja, K., Husson, L., Regard, V., Cobbold, P.R., Ostanciaux, E., Johnson, M.E., Kershaw, S., Saillard, M., Martinod, J., Furgerot, L., Weill, P., and Delcaullau, B., Relative sea-level fall since the last interglacial state: Are coasts uplifting worldwide?, Earth Science Reviews, v. 108, p. 1-15, 2011.

921. Penalver Hernandez, L, L., Castellanos Abella, E., Perez Aragon, R. O., and Rivada Suarez, R., Las Terrazas Marinas de Cuba y Su Correlacion Con Algunas Del Area Circumcaribe, Memorias Geomin, V Congreso de Geologia y Mineria, 24-28 De Marzo, La Habana, pp. 10, 2003.

922. Osmond, J. K., Carpenter, J.R., and Windom, H.L., 230 Th/234 U age of Pleistocene corals and oolites of Florida: Journal of Geophysical Research, vol. 70, pp. 1843-1847, 1965.

923. Shanzer, E.V., Petrov, O.M., and Franco, G., Sobre las formaciones costeras del Holoceno en Cuba, las terrazas Pleistocenicas de la region Habana-Matanzas y los sedimentos vinculados a ellas, Serie Geologica no. 21, Acadamia de Ciencias de Cuba, Instituto de Geologia y Paleontologia, p. 1-26, 1975.

924. Spencer, J.W., Geographical Evolution of Cuba, Bulletin of the Geological Society of America, v. 7, pp. 67-94, 1895.

925. Toscano, M.A., Rodriguez, E., and Lundberg, J., Geologic investigation of the late Pleistocene Jaimanitas formation: science and society in Castro's Cuba, Proceedings of the 9th Symposium on the Geology of the Bahamas and Other Carbonate Regions, Bahamian Field Station, Ltd., San Salvador, Bahamas. p. 125-142, 1999.

926. Vaughan, T.W., and Spencer, A., The Geography of Cuba, Bulletin of the American Geographical Society, v. 34, no. 2, pp. 105-116, 1902.

The following table in FSAR Subsection 2.5.1 will be added in a future revision of the COLA.

Table 2.5.1-208. Marine Terraces in the Matanzas Area of Northern Cuba

Marine Terrace (Reference 915)	Elevation of Marine Terrace (Reference 915)	Geologic Stratum (References 915 and 921)	Depositional Environment (Reference 915)	Possible Geologic Age (Reference 915)	Possible Geologic Age (Reference 921)
			Start of emergence	Start of the Upper Miocene	
			Erosion Cycle (No. 1)	Upper Miocene	
			Uplift and buckling (env. 60 m)	Pliocene (?)	
			Erosion Cycle (No. 2)		
			Uplift (env. 80 m)	Pliocene	
			Erosion Cycle (No. 3)		
			Uplift and folding (10 and 45 m)		
La Rayonera	25 and 51 m		Erosion Cycle (No. 4)		Pliocene-Pleistocene
			Uplift and folding (15 and 25 m)		
Yucayo	15 and 33 m		Erosion epicycle (No. 1)	Pliocene (?)	Pliocene-Pleistocene
			Drop in sea level: uplift, very light folding (10 m)	Pliocene (?)	
Puerto	16 m		Erosion epicycle (No. 2)	Start of the Illinoian Glaciation	
			Drop in sea level (11 and 13 m)		
submarine terrace	No. 1 (-1 m)		Erosion epicycle (No. 3)		
			Drop in sea level (1 m)		
submarine terrace	No. 2 (-2 and -6 m)		Erosion epicycle (No. 4)		
			Drop in sea level (env. 130 m)	Illinoian Glaciation Maximum	
Continental Shelf terrace			Erosion epicycle (No. 5)		
			Rise in eustatic sea level (+11 m)	Sangamon Interglacial	
		Jaimanitas Formation (Terraza de Seboruco), Rosario Terrace (continental alluvial terrace)	Formation of fringing reefs on uplifted alluvium deposits		Pleistocene
Limits of the Terraza de Seboruco	+/- 8 m		Drop in sea level (env. 12 m)	Start of the Wisconsinan Glaciation	
submarine terrace	No. 3 (-10 and -17 m)		Erosion epicycle (No. 6)		
			Drop in sea level (env. 10 m)		
submarine terrace	No. 4 (-20 and -55 m)		Erosion epicycle(No. 7)		
			Drop in sea level (env. 110 m)	Wisconsinan Glaciation Maximum	
Limit of the Restart of the Continental Plate			Erosion epicycle (No. 8)		
			Eustatic rise to present sea level	Flandrian Transgression	
		Recent alluvium	Induation of river valleys		

ASSOCIATED ENCLOSURES:

None